AN INNOVATIVE DESIGN OF RAINFALL SIMULATOR

FOR

MOVING STORM CONDITION

A DISSERTATION

Submitted in partial fulfillment of the
requirement for the award of the degree
of
MASTER OF TECHNOLOGY
in
HYDROLOGY
Specialization in
WATERSHED MANAGEMENT

By
RAVI KUMAR MEENA
(17537008)

DEPARTMENT OF HYDROLOGY

INDIAN INSTITUTE OF TECHNOLOGY ROORKEE

ROORKEE -247 667 (INDIA)

JUNE 2019

CANDIDATE'S DECLARATION

I hereby certify that the work which is being presented in this dissertation entitled "*AN INNOVATIVE DESIGN OF RAINFALL SIMULATOR FOR MOVING STORM CONDITION*" in partial fulfillment of the requirement for the award of the degree of *MASTER OF TECHNOLOGY* in *HYDROLOGY* submitted in the Department of Hydrology, Indian Institute of Technology, Roorkee is an authentic record of my own work carried out during the period from July, 2018 to June, 2019 under the supervision and guidance of Dr. Sumit Sen, Associate Professor, Department of Hydrology, IIT Roorkee.

I have not submitted the matter embodied in this dissertation for the award of any other degree in this or any other institute.

(Ravi Kumar Meena)

Enrollment no. - 17537008

CERTIFICATE

This is to certify that the above statement made by the candidate is correct to the best of my knowledge.

Dr. Sumit Sen

Associate Professor

Department of Hydrology

Indian Institute of Technology Roorkee

ACKNOWLEDGEMENT

I want to articulate my sincere gratitude to my esteemed supervisor Dr. Sumit Sen, Associate Professor, Department of Hydrology, Indian Institute of Technology, Roorkee for providing me an opportunity to work under his careful supervision and valuable suggestions that helped me gain fundamental knowledge and strengthened my research methodology.

Heartiest thanks are due to Dr. M. K. Jain, Dr. N. K. Goel, Dr. M. Perumal, Dr. D. S. Arya, Dr. H. Joshi, Dr. B. K. Yadav and Dr. J. Khanna for their encouragement, guidance and friendly behavior during my study.

I would also like to thank my family for their constant encouragement and support during my study period in Roorkee. It was not possible to reach till here without the support of research scholar Aliva Nanda, Bhargbnanda Dass and my friends as Pardeep, Aman, Kirtan, Nishant, Rajtosh, Gurpinder.

I am indebted to the Department of Hydrology, Indian Institute of Technology, Roorkee for constant support and help.

An assemblage of this nature could never have been attempted without reference to and inspiration from the work of others, those whose details are mentioned in the reference section. I acknowledge my indebtedness to all of them.

Last but not least, I am thankful and indebted to all those who helped me directly or indirectly in the completion of this work.

Date: June 2019 (Ravi Kumar Meena)

Place: IIT Roorkee Enrollment no. – 17537008

ABSTRACT

Rainfall simulators are widely used in the field of hydrology, biosystem engineering, agronomy, and geomorphology to understand the processes involved in these disciplines. Usually, rainfall simulators are not able to generate spatio-temporal variation in rainfall intensity simultaneously unlike natural conditions. Majority of methods used in rainfall simulator studies assumes that the rainstorm reaches instantaneously and remains steady over an area for a certain time period. Hence, most of the rainfall experiments ignore the effect of runoff response caused by moving storm across a watershed which results in under or over estimation of runoff peaks. Considering these limitations of traditional rainfall simulators, we developed an advanced rainfall simulator using eleven full cone nozzles to simulate moving front storms. These nozzles can generate rainfall intensity in the range of 55 to 780 mm/hr at a pressure range of 0.4kg/cm^2 to 1.6kg/cm^2 with a varying height from 1.5m to 4m above the ground surface. All the eleven nozzles are controlled by flow control valves and the valves are individually regulated by servo motors. Arduino Mega microcontroller system is used to control all the servo motors to generate variable rainfall intensities. Further, we have developed a mobile application for Android users to regulate all the valves of rainfall simulator. This simulator is able to simulate nearly natural rainfall conditions in the controlled environment in four different patterns i.e. uniform, advanced, delayed and intermediate. A tray of 250cm×144cm×50cm has also being designed and fabricated to conduct different hydrological experiments. This tray is designed with a provision to generate and record overland, subsurface and base flow. Tray area can also be divided in three partition to analyze three different soil conditions simultaneously. Slope adjustment, leachate collection unit and piezo metric head measurement unit are also incorporated in this experimental tray. Overall, the whole rainfall simulator with tray can be used to study the impact of moving storm on soil erosion, infiltration, and runoff in the simulated near natural environment along with pollutant transport mechanisms. This study is being focused on detailed analysis of moving storms and their impact on hydrograph characteristics. Results of this study shown a considerable difference in terms of time to peak (t_p), peak discharge (Q_p) and rescission curve for two different storm directions (upstream and downstream). Impact of this moving storm phenomena reduces with increase in storm movement velocity as well as with increase in the slope.

CONTENTS

LIST OF FIGURES

LIST OF TABLES

Chapter 1

INTRODUCTION

1.1 General

Rainfall simulation refers to the idea of simulating rain on a confined plot area for a specific time at a controlled rate. The understanding derived from rainfall simulation experiments is useful in many scientific disciplines like hydrology, bio-system engineering, agronomy and geomorphology. These rainfall simulation experiments are developed by the soil conservation service (SCS) in the 1930s to measure erodibility and infiltration capacity of the soil. The results of these experiments are used to develop the universal soil loss equation (USLE). Presently there is no universal rainfall simulator which would be applicable to all hydrological problems. During the last 40 years, many rainfall simulators have been designed. Rainfall simulation experiments have evolved with time from mere sprinkler systems to sophisticated computer-based processes involving electrical and hydraulic systems (Meyer, 1988). Rainfall simulator is classified according to the way raindrops are produced (another way of classification). The two types are (a) drip formers;(Romkens and Roth, 1977) and (b) nozzles (Meyer & Mccune, 1958). Drip formers are used for small plot area and for low intensity rainfall studies (Regmi & Thompson, 2000; Foster et al., 2000). Pressurized nozzle (Meyer & McCune1958)(Norris P. Swanson, 2013) (Hall, 1970) is used commonly for large scale field studies (10 to 500 m^2).

1.2 Application

Due to high variability in natural rainfall, it is difficult to study its characteristics and its impact on overland flow and soil erosion at watershed-scale. Thus, rainfall simulators are employed to study hydrological processes under controlled rainfall condition. The application of rainfall simulator is to collect runoff, infiltration and erosion data in both field and laboratory scale experiments. The use of rainfall simulators in urban hydrology studies is relatively recent. Lima and Singh (2002) used single nozzle rainfall simulator for moving storm analysis and (Egodawatta et al., 2009);(Miguntanna et al., 2010) (Liu et al., 2013)used a rainfall simulator which was developed by Herngren (2005), for pollutant build-up and wash-off processes, and for urban water quality research. Results obtained from these experiments helped in understanding the slope-soil

properties and the effect of surface resistance (i.e. vegetation and micro-topography conditions) on overland flow and infiltration processes. Moreover, it can also be useful to study the flow routing, sediment generation and transportation at different scales i.e. plot-scale (Nanda et al., 2017) to hillslope-scale (Hall, 1969).

1.3 Problem statement

Usually, rainfall simulator allows the controlled application of water on a certain plot area to mimic the natural rainfall and to study the rainfall-runoff characteristics. However, rainfall simulator fails to replicate the natural rainfall accurately (Singh, 1998) due to constraints related to cost and simplicity. Most of the times rainfall simulator is not able to produce variable intensity rainfall both spatially and temporally, simultaneously, unlike natural rainfall. In most of the rainfall simulation studies, rainfall intensity is taken as a constant parameter for a particular area at an instant of time (Singh, 1998) but in natural rainfall condition, rainfall intensity varies rapidly over space and time.

The spatio-temporal distribution of rainfall influences the overland flow characteristics (Singh, 1998; Lima and Singh, 2002) nevertheless, majority of methods used in hydrological studies assumes that the rainstorm reaches instantaneously over the watershed and remains steady over it. Thus, these hydrological studies ignore the effect of storm movement on watershed runoff response. Excluding the storm movement, could lead to poor estimation of runoff peaks (Wilson et al., 1979).

1.4 Objectives

Hydrograph generated at an outlet of a catchment by considering different scenarios of storm movement direction exhibits unique characteristics especially in terms of peak flows, time to peak and recession curve of the hydrograph. Furthermore, storm movement velocity and basin slope also influence the shape of the hydrograph. But it is difficult to analyze the moving storm characteristics under natural rainfall condition. Considering this, the following specific objectives were studied to understand moving storm behavior under artificial rainfall condition.

1) Design of rainfall simulator for moving storm condition
2) Analysis of moving storm hydrograph

The rainfall simulator comprises of three stages of the design process. Starting with the assembly of servo motor operated valve placed before the nozzle to control the flow through it. Then using a microcontroller to regulate all the valves simultaneously and finally with the aid of a user interface, a moving storm condition was simulated. The moving storm hydrographs were generated on a saturated plot for the following conditions:

a) Two different slope conditions (2.5% & 5%)
b) Two different directions of storm movement (upstream and downstream)
c) Three different storm movement velocities (2 m/min, 3 m/min and 6 m/min)

Chapter 2

LITERATURE REVIEW

2.1 Impact of moving storm on different hydrological parameters

De Lima and Singh, 2002 studied the nonlinear kinematic wave approach to analyze the impact of both storm pattern and storm movement on hydrograph characteristics. Four different storm patterns named as uniform, intermediate, advanced and delayed as shown in Figure 2.1 was used. Six different velocities were used for simulations with effective rainfall intensity of 30 mm/h over the plot of 1 m width and 100 m length with a uniform slope of 10 % and storm direction considered towards both upstream and downstream. Different sets of experiments were conducted by varying one parameter at a time while keeping the others constant. From these simulation experiments, authors concluded that the hydrograph shape and peak discharge strongly depends on storm pattern, storm movement velocity and storm movement direction. Storm moving downstream are normally characterized by hydrograph with delayed rise, high peak discharge, steep rising limb and short base time.

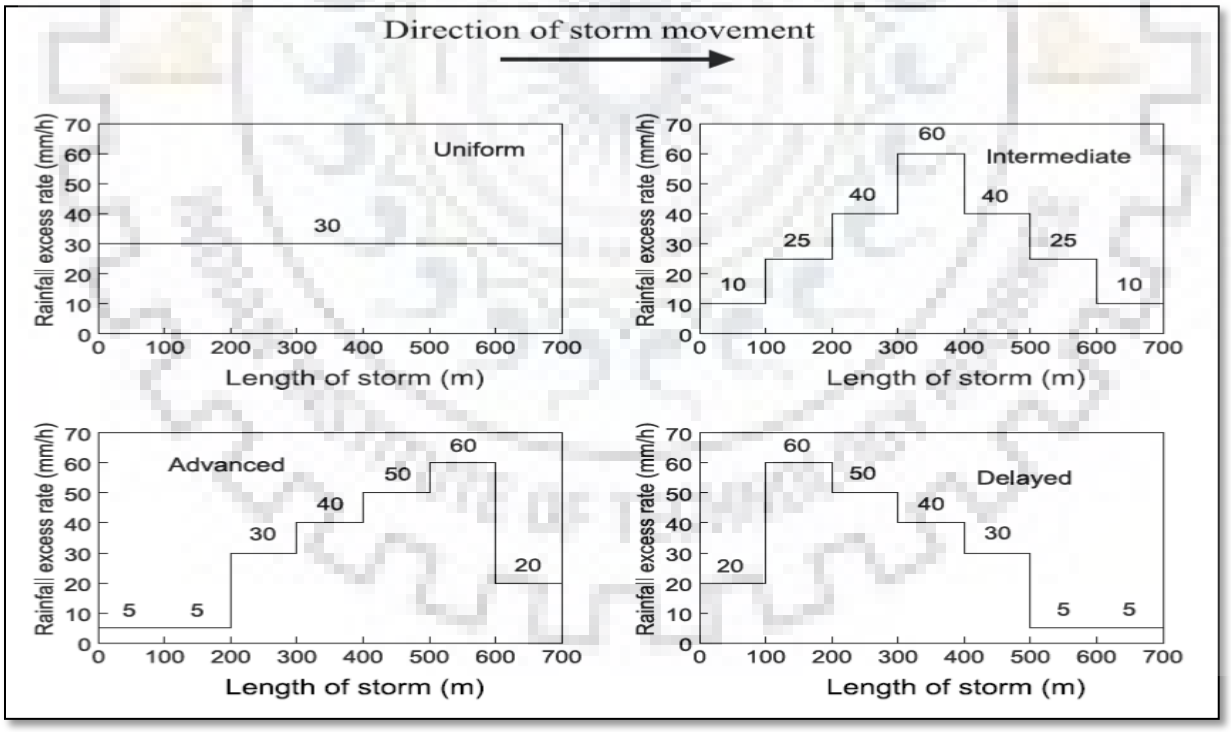

Figure 2.1 Spatial rainfall patterns Source: Advances in Water Resources 25 (2002) 817–828

Lee and Huang, 2007 studied the impact of moving storm on steady-state discharge condition in two types of basin geometry i.e. plane and V-shaped (Figure 2.2). A fixed dimensional analysis was used to calculate autonomous variables which govern the systematic sequential numerical simulation. Results of this research showed that downstream moving storm achieved equilibrium discharge state also at a shorter storm length as compared to catchment length. But an upstream moving storm required a longer storm length to achieve an equilibrium discharge state. Process of achieving equilibrium discharge state for moving storm scenarios controvert the basic hydrology as it takes rain storm duration to be equal or greater than the equilibrium time for that watershed.

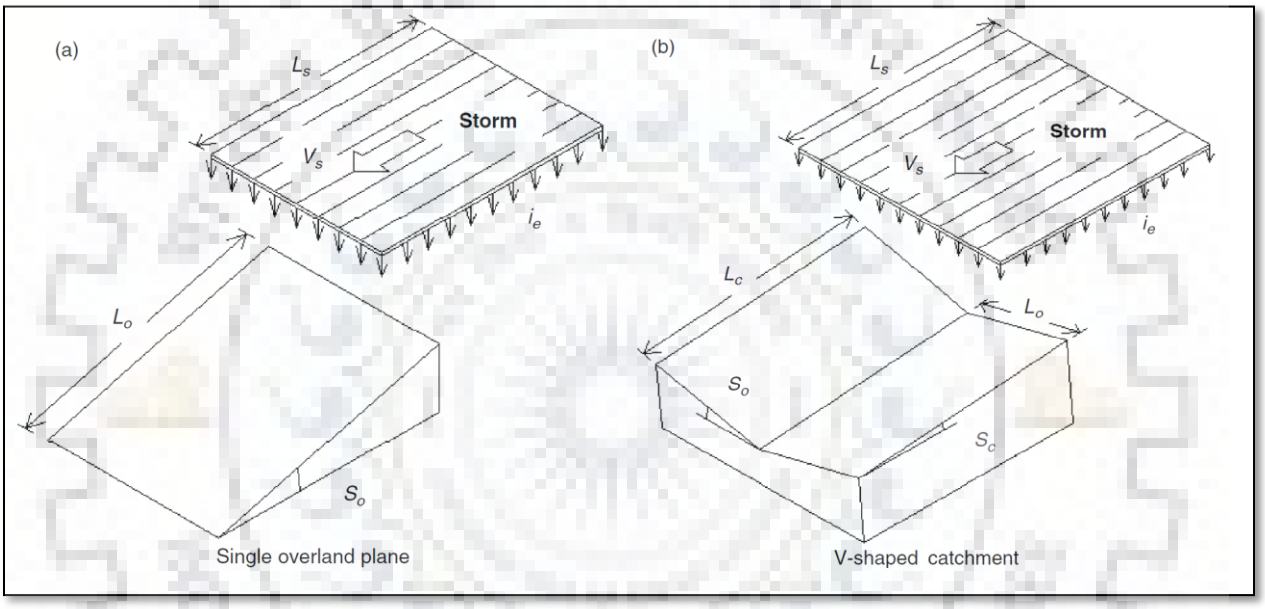

Figure 2.2 Downstream-moving storm on two different topography of catchment: (a) single overland plane; (b) V-shaped catchment

Seo and Schmidt, 2012 studied a variety of drainage setups by taking rectangular basin under consideration. As the urban drainage efficiency varies as compared to natural drainage system, thus different drainage setups were simulated through Gibbs model. For reference, they used an equivalent evenly spread rainfall over the catchment used for the experiment. Both upstream, downstream moving storms with different storm velocity were used in this analysis. They concluded that the relation between the storm velocity, direction of storm movement and peak flow depends on drainage setup and its efficiency.

(Seo and Schmidt, 2014) conducted their research on a synthetic drainage area of the circular shape to remove the impact of basin geometry, and they analysed the rain storm peak for a particular drainage network and compare the result of both moving storm as well as stationary storm. Peak discharge for moving storm scenario was higher than the equivalent stationary storm. Bad drainage system did not respond well to the effect of moving storm as compared to a well-developed drainage system. Peak flow for a moving storm depends on many parameters such as storm velocity, rainfall intensity, the direction of storm movement and also on the properties of the drainage system. This research work purposed that the urban drainage systems should be designed by taking storm movement and its impact on peak flow under consideration for construction of a safe and efficient drainage system.

2.2 Use of rainfall simulator for moving storm analysis

De Lima and Singh, 2003 studied the impact of moving storm on water-induced soil erosion from sloping land. For this study, a sprinkler type of rainfall simulator was used with a support structure to move the simulator in forward and backward direction with the help of electric motors. Nozzle height and water pressure for the nozzle was 1.5 m and 50 kpa and remained constant for all the experiments (Figure 2.3). The effect of wind on rain drops was excluded. Soil flume used for this experiment was of metal sheet with dimensions of 2.0 m x 0.1 m x 0.12 m and no buffer zone was provided around flume to compensate for water and soil splashed outside the flume. For the simplicity of simulated rainfall pattern, the width of soil flume was taken small. Two different sets of experiments were done in this study. In the first set 13 replicates of upstream movement and 13 replicates of the downstream movement were taken with five different slopes at a constant velocity of 0.33 m/s. And in the second set of experiments, 62 replicates with 23 different storm velocities with a constant slope of 10 % were performed. The results concluded that water-induced erosion is highly dependent on spatio-temporal rainfall distribution. The upstream storm movement yields less soil loss as compared to the downstream moving storm which is markedly influenced by hydrograph characteristics of overland flow. The bed slope has a direct relationship with soil loss in both conditions of storm movement whereas storm movement velocity has an inverse.

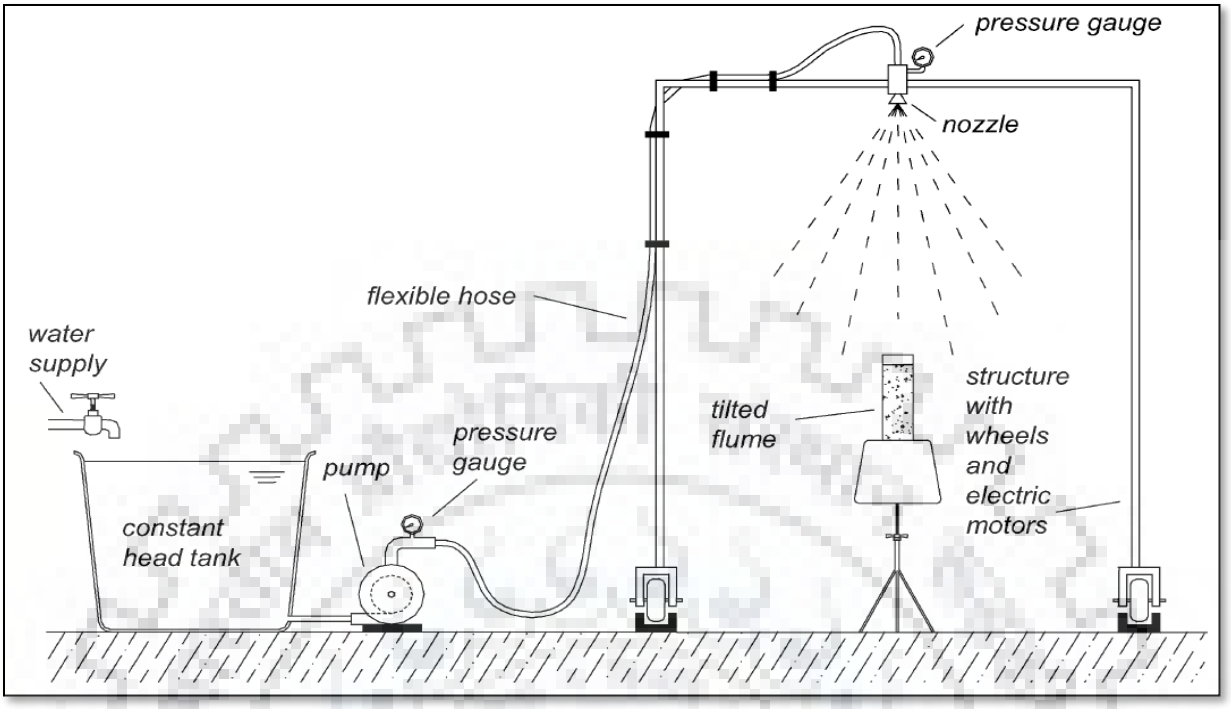

Figure 2.3 Schematic of rainfall simulator for moving storm simulation. Source: Physics and Chemistry of the Earth 28 (2003) 277–282

De Lima et al., 2003 used a movable sprinkler rainfall simulator to simulate a moving storm and lab experiments were conducted to assess the effect of a moving storm on overland flow. Overland flow conditions for moving storms are non-linearly varying processes and significantly differs for stationary storms considering spatio-temporal distribution of the rainfall. The study validates the fact that the effect on flows owing to storm movement has long been known but most hydrological study methodology proceeds assuming instantaneous stationary storm over the drainage plots. This might often result in the poor estimation of runoff peaks. The rainfall simulator in this study benefits the author in being versatile as it provides spatio-temporal control on precipitation characteristics in both field conditions and laboratory setups. The study stresses that in windy environmental setting the non-uniform components of the simulated precipitation like rain intensity pattern, spatio-temporal variance, incident drop angles and size of droplets considerably affect the overland flow hydraulics.

The rainfall simulator used for the experiments was portable, capable of moving back and forth simulating storm movement and had dual electric motor supporting the downward oriented conical

nozzle and spraying continuously. A constant head tank and a stable pressure pumping system was connected to the nozzle. The simulated rainfall has a constant intensity being monitored by a pressure gauge. The study only used a single nozzle at a fixed height above the metal tray or the impermeable surface used to monitor overland flow. The experimental results for downstream moving storm state that runoff commencement at the lower end of the tray is much dependent on the velocity of storm and surface flows. If storm velocity is greater than surface flow velocity there will be a delay in water contributed from upstream areas of the tray surface. If the movement of the storm is in the upstream direction, the runoff beginning at the low end of the surface is less influenced by storm velocity and overland flow (Figure 2.4). The study concludes that slower storm movement produces a higher volume of runoff, heightened discharge peaks and prolonged base periods whereas faster moving storms result in a lesser amount of runoff and the negligible difference in storm hydrographs moving in the two opposite directions. Higher peaks in discharges have been observed for downstream moving storm compared to the same rainstorm moving upstream for the same velocity.

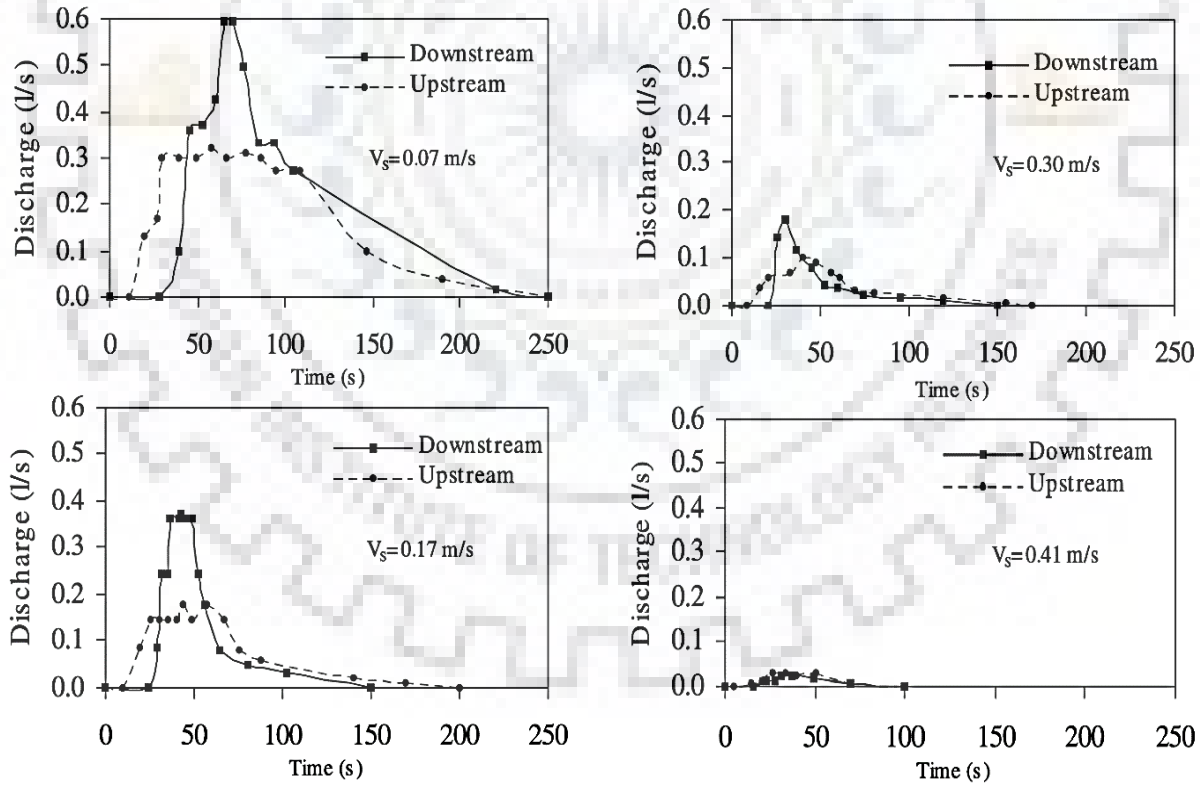

Figure 2.4 Effect of direction of storm movement on measured hydrographs for 4 storm velocities. *Source: Physics and Chemistry of the Earth 28 (2003) 277–282*

De Lima et al., 2009 studied water-induced erosion and overland flow analysis, the nonlinear impact of moving storm on hydrological response is unaccounted for even after knowledge of storm movement's significance on overland flows have long been established, this is owing to increase in complexity of models. This is contrary to natural precipitation which varies highly at both spatial and temporal scale. Neglecting the storm movement considerably affects the quantity of runoff peak estimation and sediment transport processes. The prime objective of this work was to analyze the effect of storm movement direction on soil erosion in slopes and superficial flows. The experiments conducted employed a circular soil flume to isolate the direction variability of the rain storm as a circular flume will render the rainfall input to have a constant duration and depth regardless of storm direction and storm events. Experiments were conducted using a movable type sprinkler system rainfall simulator on a soil flume of circular dimension and analyzing the runoff hydrograph and sediment graph observed for varied simulations (Figure 2.6). The circular flume, had a 2.0 m diameter and 0.10 m width of the buffer zone along the circumference compensating for splash induced water and sediment ejection. The flume soil comprised of a combination of clay, silt and sand in the ration of 11:10:79 and the bed slope provided was 10 %. The rainfall simulator had full cone nozzles spaced equally and oriented downward placed in a movable support structure with water connections and pump systems. The simulated rain droplets had a median diameter of 1.5 mm. The storm movement was simulated for five-movement directions and five speeds for each direction (Figure 2.5). The results concluded that a downstream moving storm has greater potential then upstream moving storm in terms of overland flow discharge and sediment yield (Figure 2.7).

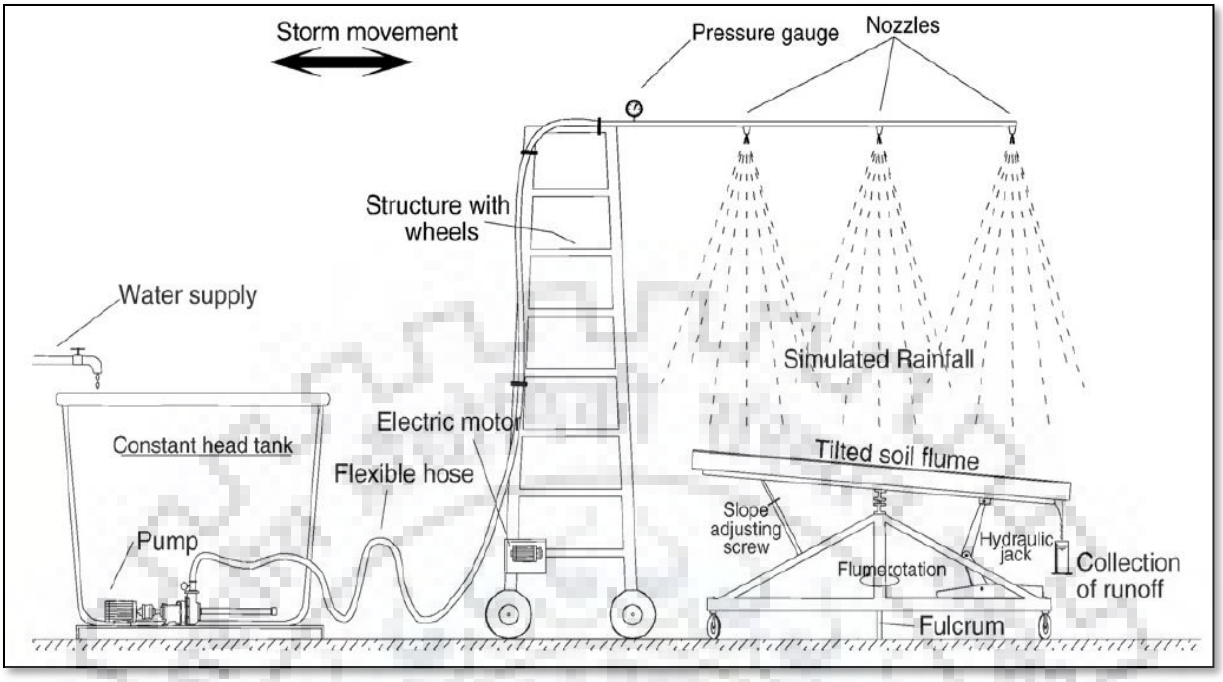

Figure 2.5 Schematics of the laboratory experiments. Source: Geoderma 152 (2009) 9–15

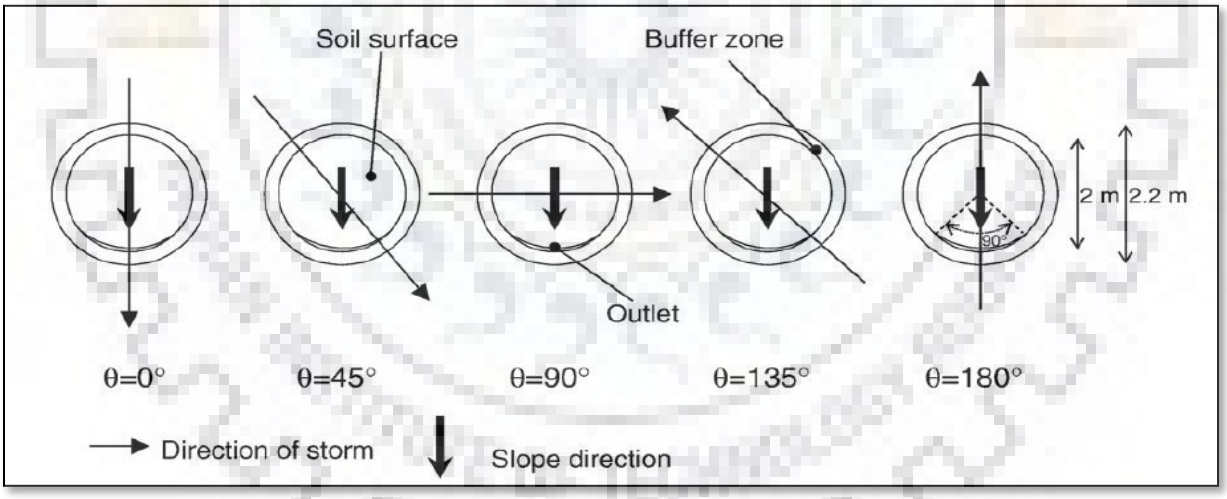

Figure 2.6 Five storm directions used in the laboratory experiments. θ is the angle between the storm direction and the slope direction. Source: Geoderma 152 (2009) 9–15

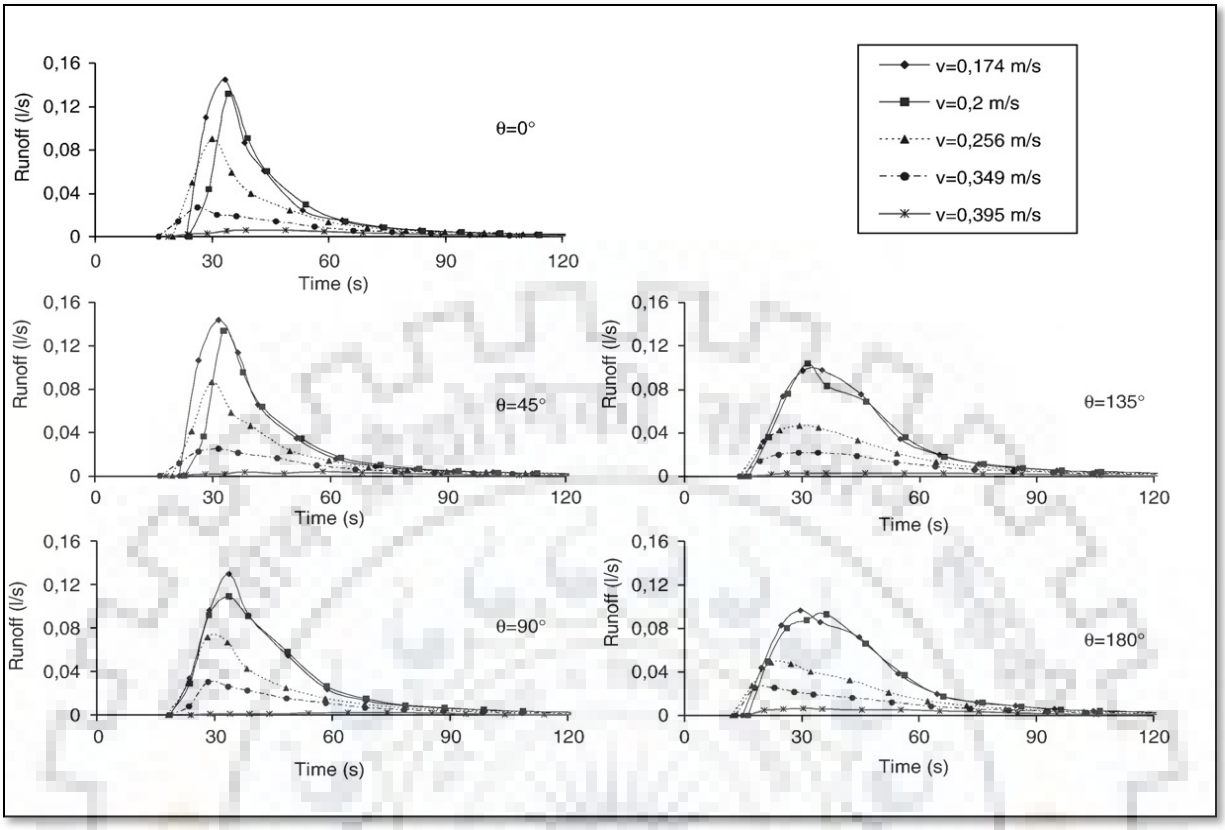

Figure 2.7 Runoff collected in time for all experimental runs (25 events, 5 storm directions and 5 storm speeds) Source: Geoderma 152 (2009) 9–15

De Lima et al., 2011 this research work was focused in determination of soil grain size transported by runoff generated by constant speed rain storm at different slope condition and different directions of storm movement. For this study, a single nozzle rainfall simulator is used which have a motor operated wheel base to move the simulator at a desired speed over a tray of area 0.9 m^2 (Dimension - 3.0 m×0.30 m×0.10 m) with a provision to change slope as per requirement. Rainfall simulator was maintained at pressure of 2 bar to simulate an average rainfall intensity of 138 mmh^{-1}. Experiments were carried out to prove that there is a variation in the amount and particle size of the soil transported by runoff due to the direction of storm movement, experiments are carried out at three different land slope and two storm movement direction (downstream and upstream). Results of this study show that downstream moving storm causse more sediment transport then upstream moving storm, also the particle size of the soil eroded is coarse in the case of downstream moving storm (Figure 2.8).

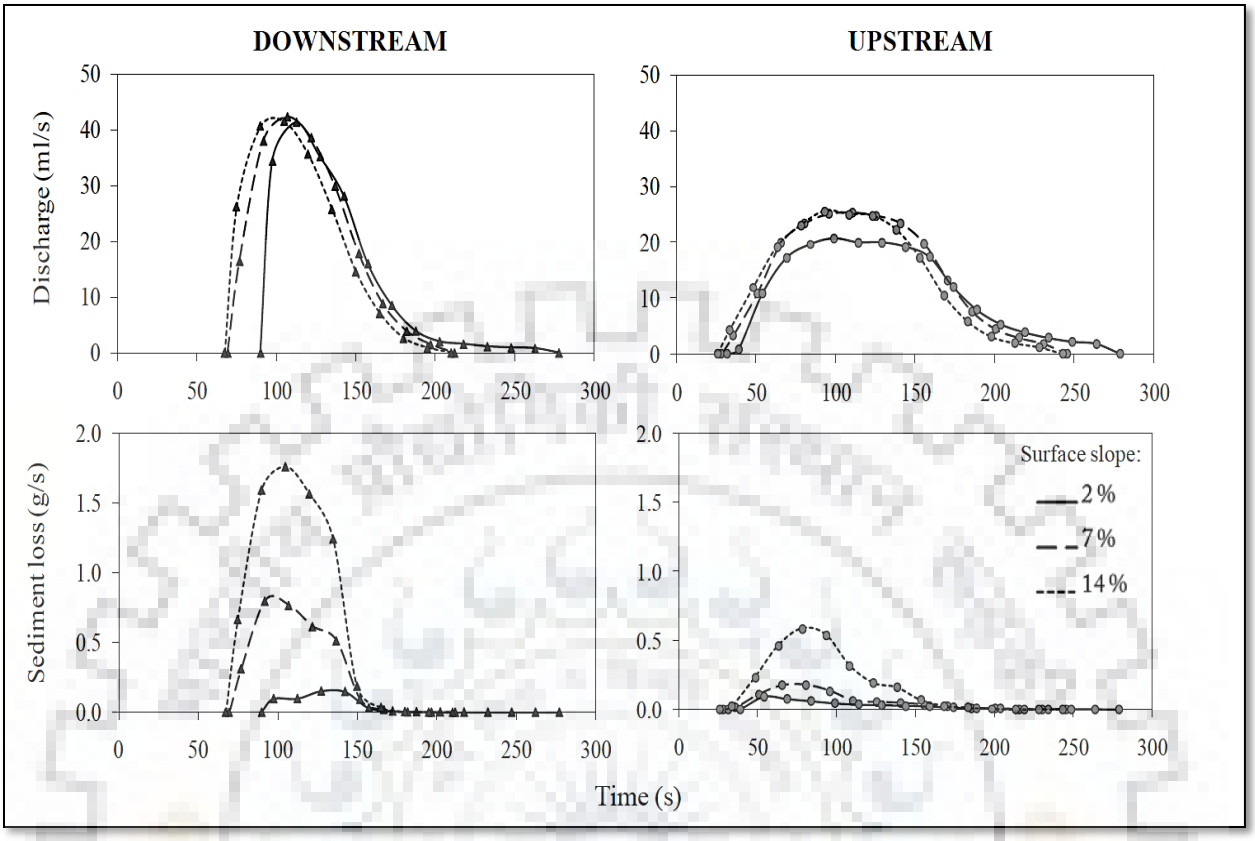

Figure 2.8 Runoff hydrographs and sediment graphs for three different slope condition and two storm movement direction. Source: www.nat-hazards-earth-syst-sci.net/11/2605/2011/

Cai et al., 2012 proposed a computer based programmable logic control system (PLC) to operate a rainfall simulator, with a user friendly interface to operate the system (Figure 2.10). This study was focused on designing a single nozzle rainfall simulator in which any rainfall intensity within a certain range can be simulated, also able to generate variable rainfall intensity over the plot area (Figure 2.9). The PLC developed for this system works through a frequency pulse-based signal within the range of 480 ms to 2400 ms and to operate the PLC a computer is required for man-machine interaction. This operating system is designed in such a way that one can keep track of rainfall intensity throughout the simulation and can change the controlling parameters as per requirement. For the evaluation of the rainfall simulator, a procedural 6 selected working states were defined and experiments were conducted, and rainfall uniformity was estimated by dynamic and static multi-nozzles. The estimated uniformity of simulated rainfall is in the range of 0.89 to 0.93.

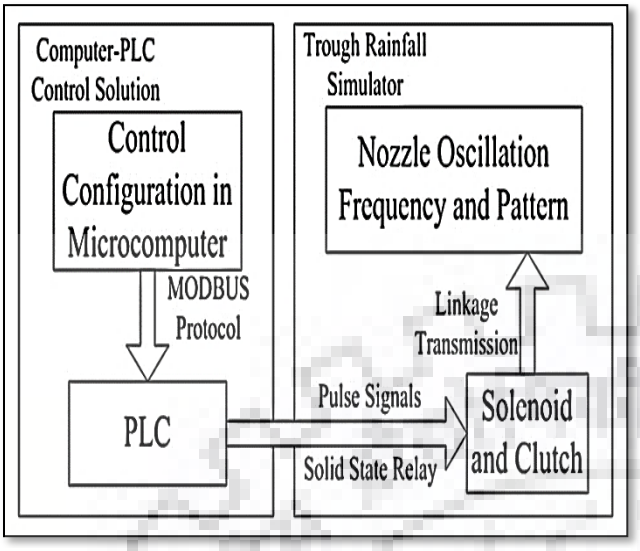

Figure 2.10 Structure of computer-based PLC control simulator Source: IEEE (2012) 978-1-4673-1398-8/12

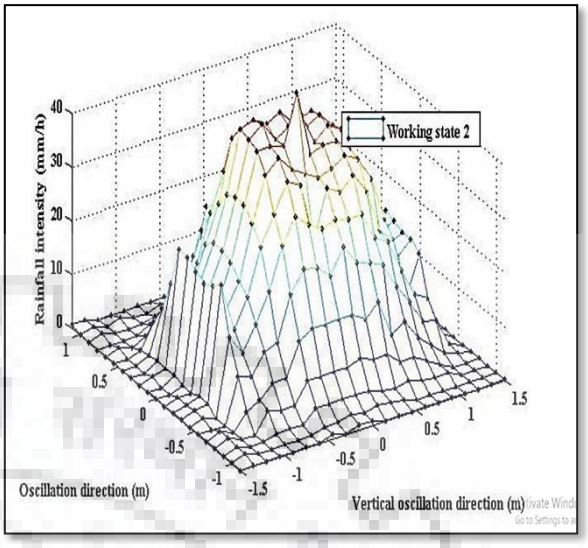

Figure 2.9 Single nozzle rainfall modeling result of working state 2 Source: IEEE (2012) 978-1-4673-1398-8/12

Ran et al., 2013 used a multiple hypodermic needles based movable rainfall simulator was employed over a plot of 4m x 1m used to simulate moving storm, tray have silty sand, equipped with a moisture sensor, a discharge measurement setup and also have provision to change the slope of the tray (Figure 2.11). Simulated rain storms have three combinations of rainfall intensity and storm duration was used with an average storm movement velocity in the range of 0.2×10^{-3} m/s to 4.4×10^{-3} m/s. In this research work they concluded that the rainfall-runoff and sediment transport process strongly depends on rainfall intensity and the total amount of rainfall, higher intensity rainfall have more significant for both upstream and downstream storm movement over the runoff characteristics as compared to sediment transport. Canonical correlation analysis shows more significant results in the case of a downstream moving storm.

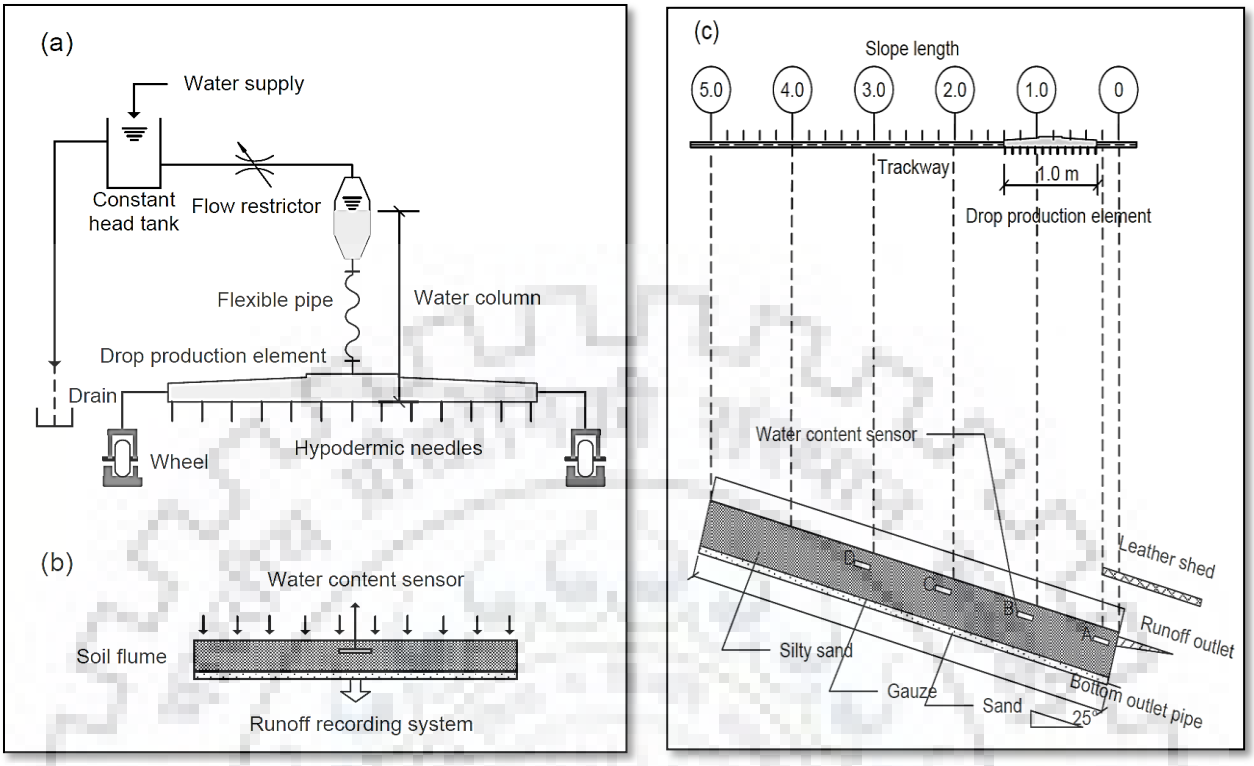

Figure 2.11 Schematic diagram of the laboratory set-up (a) rainfall simulator; (b) tray; (c) Elevation of main frame. Source: Ran et al. / J Zhejiang Univ-Sci A (Appl Phys & Eng) 2013 14(5):353-361

2.3 Other approach used for moving storm analysis

Sigaroodi and Chen, 2016 conducted this research near international borders of Iraq-Iran-Turkey, sub-catchment of Lake Urmia of area 1146 km^2, this area is divided into 7 sub-basins. This part of the catchment of Lake Urmia is mostly mountainous and have the cover of farmland, grassland and orchards. This study was carried out by comparing the resulting hydrographs of consideration of stationary and moving rainfall to the observed hydrographs. Hydrographs for stationary rainfall were based on the nearest rain gauge hyetograph and the hydrographs for moving storm condition were based on moving hyetograph estimated on the basis of logged timing of hyetograph in the basin. Results showed that the hydrographs of moving storm were similar to the observed hydrographs as compared to the stationary rainfall hydrographs (Figure 2.12).

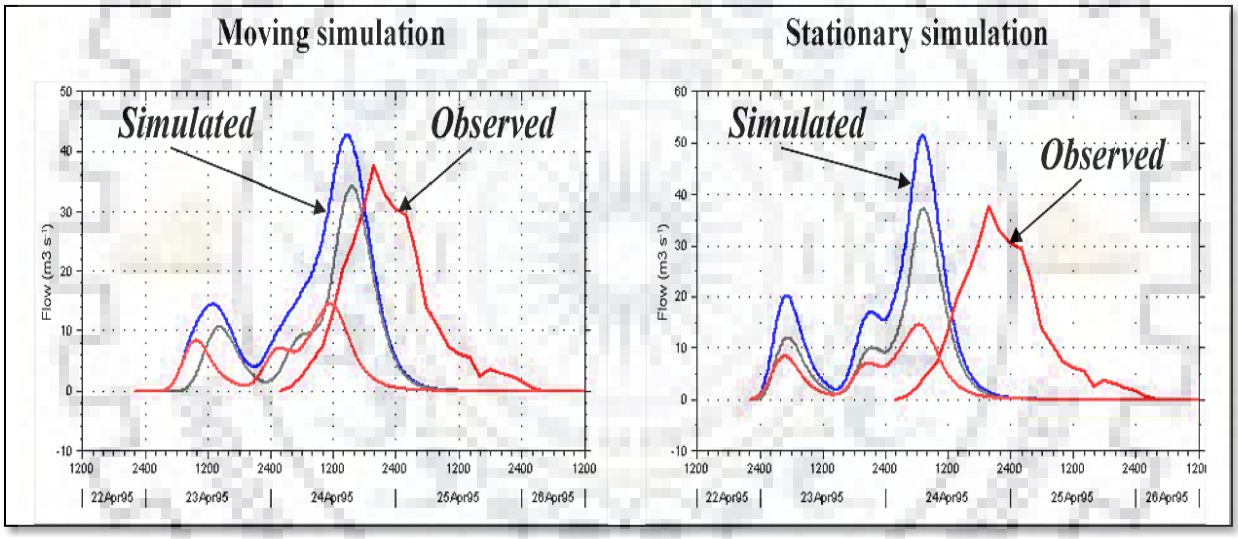

Figure 2.12 HEC-HMS output for two different conditions Source: www.hydrol-earth-syst-sci.net/20/5063/2016

Lee et al., 2015 majorly focused on three typhoons of the last decade which have a large impact on the South Korean economy and caused considerable life loss. They proposed a different approach to analyze the impact of storm movement and its direction of movement over watershed scale, instead of changing storm direction they suggest to rotate the basin 180° to analyze the impact of the downstream and upstream movement of rain storm. Radar data of meteorological station of Jindo was used which is situated near the Basin of Nam River. In this research work, they also check the different basin response to the different storm direction, and its impact on flow prediction, sediment transport and watershed management policies.

Table 2.1 Comparisons of rainfall simulator experimental configurations in key research papers.

Key Papers	Soil Composition	Slope (%)	Storm Movement Direction	Rain Intensity (mm/h)	Storm Movement Velocity (m/s)	No. of Rainfall Patterns
J.L.M.P. de Lima et al., 2009	11:10:79 (clay:silt:sand)	10	Five (θ = 0°, 45°, 90°, 135°, 180°)	180	0.174 – 0.395 (Five different)	1
J.L.M.P. de Lima, V.P.Singh., 2003	Non-infiltrating	5	Two (U/s and D/s)	320	0.07 – 0.41 (Four different)	1
J.L.M.P. de Lima et al., 2003	11:10:79 (clay:silt:sand)	5, 10, 15, 20, 23 (five different)	Two (U/s and D/s)	498	0.1 – 0.7 (twenty-three different)	1
J.L.M.P. de Lima, V.P.Singh., 2002	Non-infiltrating	10	Two (U/s and D/s)	30	0.5 – 5 (Six different)	4

Chapter 3

MATERIAL AND METHODOLOGY

The rainfall simulator used in this study was designed at the Department of Hydrology, IIT Roorkee. The instrument consists of 3 m x 2 m frame connected with a PVC pipe attached with header (supporting 11 nozzles) and pressure gauge. Frame supported by four telescopic legs of 4m each (Figure 3.1). The rainfall structure is connected to a centrifugal pump capable of controlling the water pressure and lifting up the water from a tank near the pump. The main components of the simulator are: (a) Frame; (b) Header for nozzle mounting; (c) Nozzles and (d) Pumping station. The system is supplied with water pumped from a storage tank located near the plot. Water pressure in the system can be adjusted by a pressure regulator, and by applying back pressure on the outflow end of the simulator system by means of a "shut-off" valve. Another valve has been used to facilitate accurate control of water pressure for the nozzles.

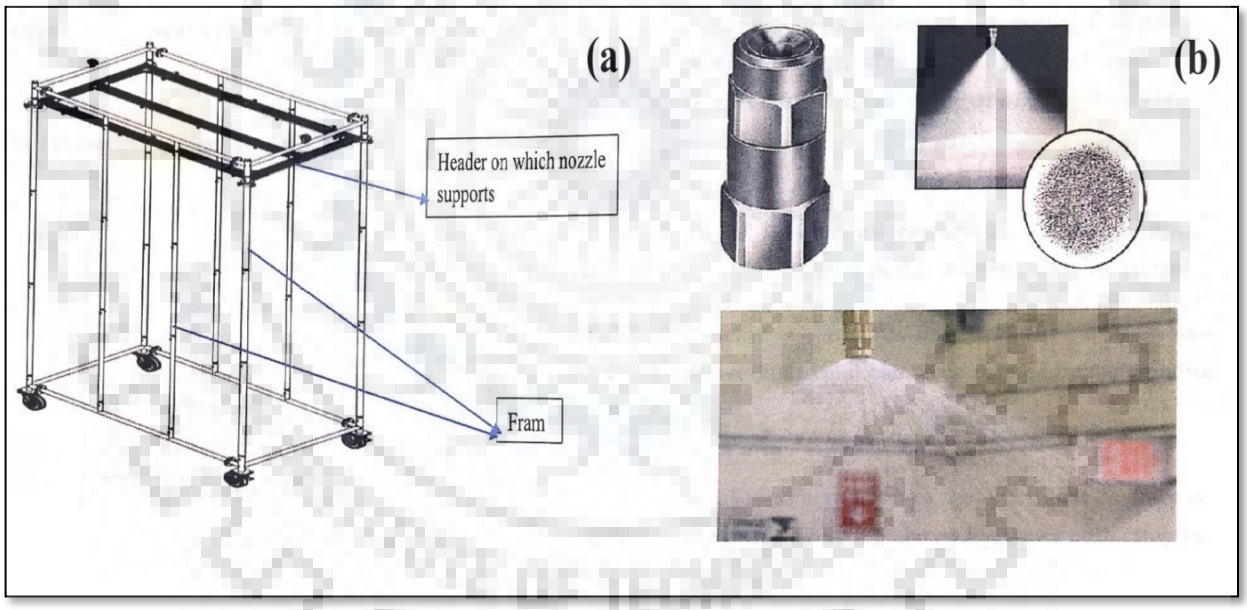

Figure 3.1 (a) Schematic diagram of rainfall simulator. (b) Spraying System Co. Full jet G-style Spray Nozzle and Nozzle Spray flume. Source: spraying system co. pvt ltd, Bangalore

Six full-cone nozzles manufactured by Spraying Systems Co. are available: B1/88G-SS4.4W, B1/4GG-SS10W, B1/4GG-SS414W, B3/8GG-SS17W, B1/2G-SS30W and B1/2GG-SS40W arranged from small to larger size used to simulate low to high intensity rainfall respectively. These

nozzles produce a solid cone-shaped spray pattern with a round impact area of medium to large sized drops (Figure 3.1). Uniform Spray coverage and distribution over a wide range of flow rates and pressure is possible. B1/88G-SS4.4W is used for this moving storm study. Some models include removable caps and vanes for easy inspection and cleaning, as well as several other mounting options.

Table 3.1 Specification for nozzles available for rainfall simulator

Nozzle	Orifice diameter (mm)
B1/88G-SS4.4W	2
B1/4GG-SS10W	2.8
B1/4GG-SS14W	3.6
B3/8GG-SS17W	4
B1/2G-SS30W	5.6
B1/2GG-SS40W	6.4

3.1 Design of soil flume

A flume of 2.5 m * 1.44 m * 0.5 m of stainless steel having thickness 2.5mm is developed for soil bed preparation (Figure 3.2). Acrylate sheet is provided at one side of the soil flume for visibility. For support iron angles of 5mm thickness are used. The base frame of 0.5 m height is designed for the stability and to support the jack system. Manually operated worm wheel gear jack setup is installed to change the slope of the flume. Flume has three sub partitions to accommodate three different soil types at a single time. At downstream of the flume, outlets for surface flow, sub-surface flow and base flow measurements are given. The surface and subsurface flow outlets are placed at a height of 50cm and 25cm from the bottom of the flume, respectively. The outlet for baseflow measurement is located at the bottom of the flume. Moreover, ten 5mm diameter slots are provided at each sub partition to analyze the change in piezometric head. These slots can also be used for leachate studies.

At first, the soil flume was filled with gravel up to 5cm depth to prevent the movement of soil. The sand was placed above the gravel bed to a depth of 2.5cm and then the remaining 42.5cm flume space was filled with the soil (Figure 3.3). The sand, silt and clay composition of this soil is 66%, 29% and 3%, respectively.

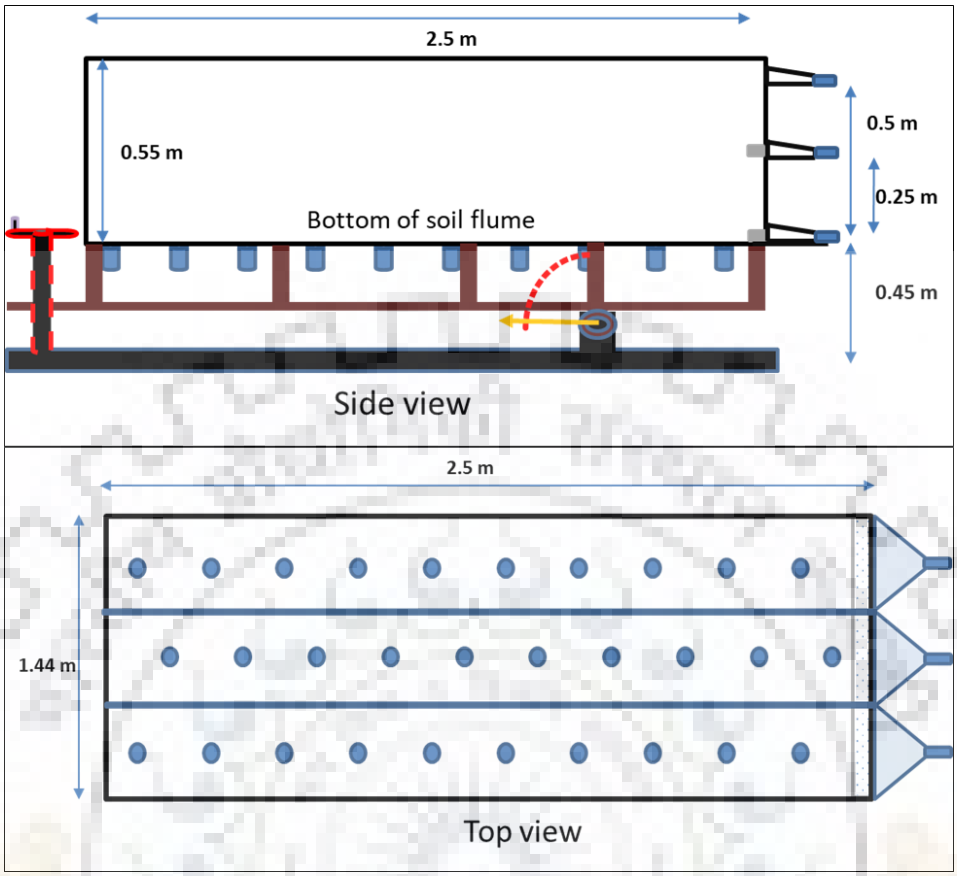

Figure 3.2 Design of soil flume

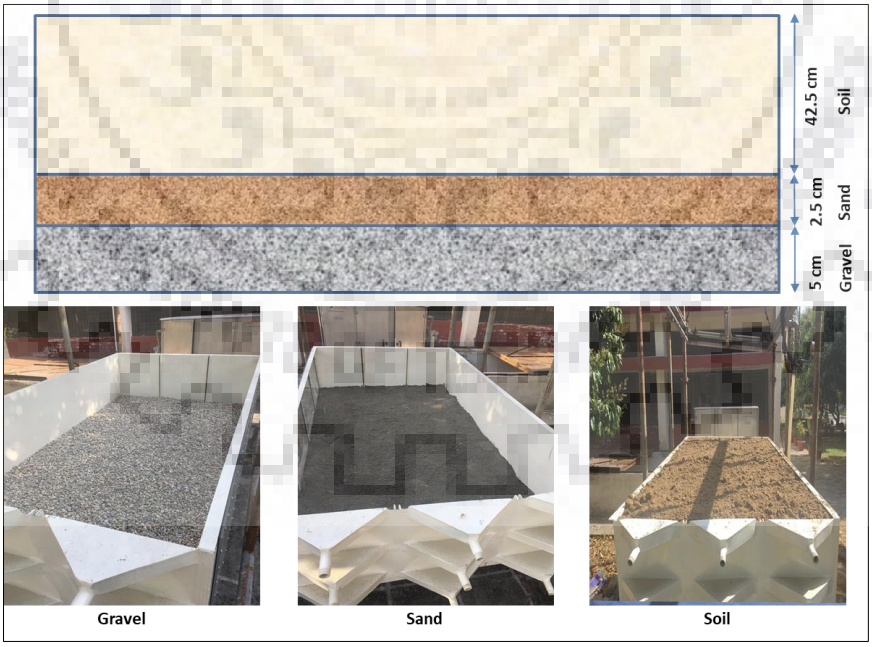

Figure 3.3 Filling materials used in soil flume

3.2 Moving Storm Condition

For the simulation of moving storm condition, all 11 nozzles are to be controlled by electrically operated flow control valve through a microcontroller board system (Arduino Mega) which can control the flow of all 11 nozzles simultaneously. Nozzles are divided into four groups 3, 3, 3 and 2. These groups are activated and deactivated with a certain time gap to simulate moving storm over a plot area. To obtain variable rainfall intensities, servo motor operated flow control valve is inserted in the pipe just before the nozzles. Servo motors are operated through microcontroller board and for easy control, Bluetooth module is used. Further, we have developed an Android mobile application for opening and closing of the valves.

3.3 Uniformity coefficient

The uniformity coefficient was measured using 66 beakers kept in a square array, 0.25 m apart, beneath the simulator, covering the plot area of 2.5 m x 1.44 m. The *Christiansen Uniformity Coefficient* (CU) was used to evaluate the uniformity of the simulated rain. The CU is defined as the deviation of individual observation from mean over the mean value and number of observation (Herngren, 2005) and can be calculated by the equation (1)

$$\mathrm{CU} = 100\left[1 - \frac{\sum_{i=1}^{n}|X_i - \mu|}{\sum_{i=1}^{n} X_i}\right] \qquad \text{Equation (1)}$$

where μ is the average of all the measurements, $|X_i - \mu|$ is the sum of the individual deviations from the mean, and n is the number of measurements taken.

3.3.1 Rainfall intensity

Rain-wise tipping bucket rain gauge is used for the estimation of rainfall intensity (Manufactured by Rain-Wise, USA). It consists of a funnel that collects water drop into a small seesaw-like container as shown in Figure 3.4. After the pre-set amount of rainfall falls, the lever tips and dumps the collected water and send an electrical signal to rain log data logger.

Figure 3.4 Rain wise tipping bucket rain gauge

3.4 Hardware used and its operational functioning

3.4.1 Servo operated valve

A stop cock valve is used to develop a servo-operated valve due to its low operational torque requirement. Servo motor of torque 10 $kgcm^{-2}$ which is easy to control and have fairly high accuracy is used to control the valve. An aluminium frame is designed using a 2.5 mm aluminium sheet to hold servo motor and stop cock valve together (Figure 3.5).

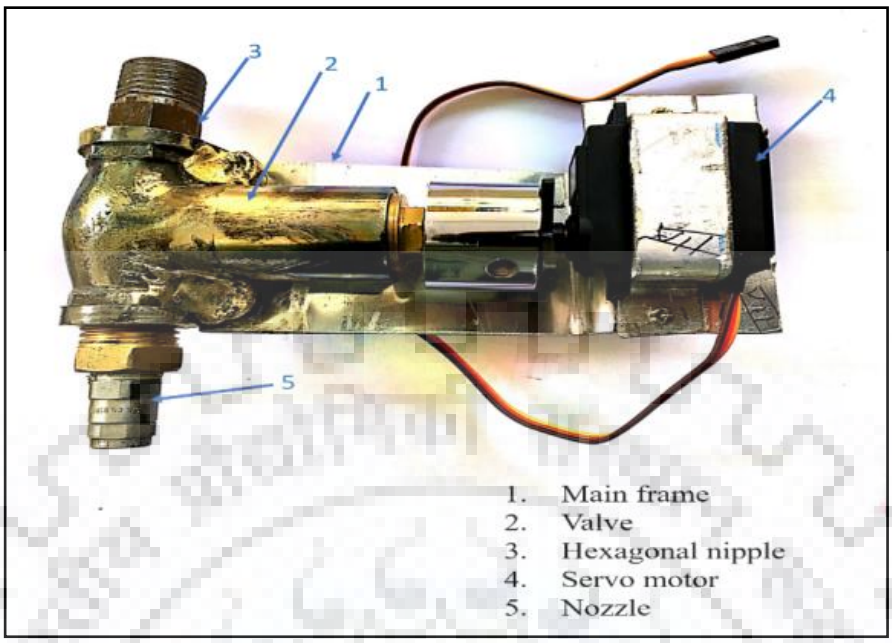

Figure 3.5 Servo operated valve assembly

3.4.2 Arduino Mega

Arduino Mega (Figure 3.6) is a microcontroller board having fifty-four digital I/O pins, four hardware ports, sixteen analog ports and a 16 MHz crystal oscillator complemented by an ICSP header, a power jack and a reboot button (Table 3.2). It can be powered through both USB as well a DC supply of 7-12 V 1A. It can be code by an online Arduino editor web site or by windows based Arduino editor software. C/C++/Python can be used as a coding language to code microcontroller which makes it easy to use as per requirement.

Table 3.3 Specification of Arduino Mega. Source: - www.arduino.cc

Sr. No.	Pin Number	Pin Description
1	D0 – D53	54 Digital Input / Output Pins.
2	A0 – A15	16 Analog Input / Output Pins.
3	D2 – D13	12 Pulse Width Modulation (PWM) Pins.
4	Pin # 0 (RX), Pin # 1 (TX) Pin # 19 (RX1), Pin # 18 (TX1) Pin # 17 (RX2), Pin # 16 (TX2) Pin # 15 (RX3), Pin # 14 (TX3)	4 Serial Communication Ports (8 Pins).
5	Pin # 50 (MISO), Pin # 51 (MOSI) Pin # 52 (SCK), Pin # 53 (SS)	SPI Communication Pins.
6	Pin # 20 (SDA), Pin # 21 (SCL)	I2C Communication Pins.
7	Pin # 13	Built-In LED for Testing.

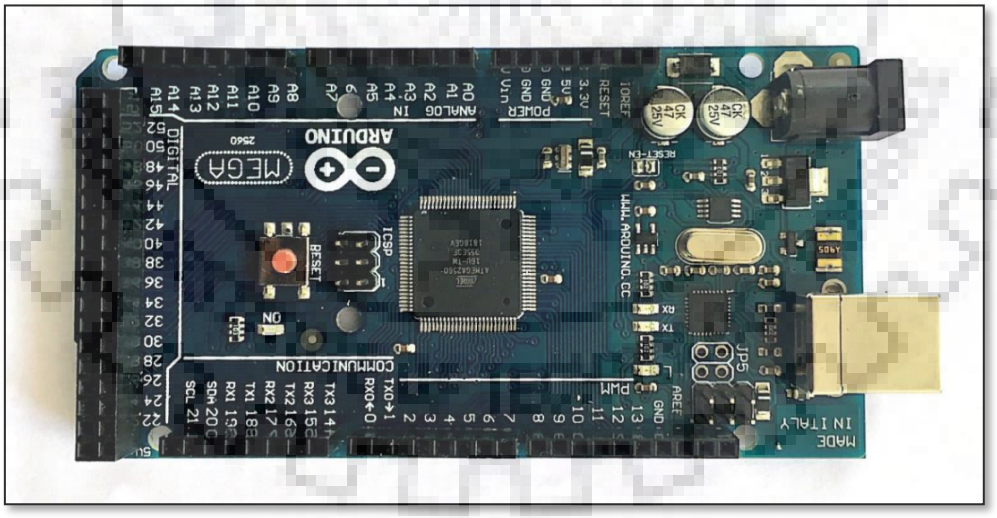

Figure 3.6 Arduino Mega

3.4.3 Servo Motor

Servo motor MG995 is a High-Speed Digital Motor having a rotation angle of 90° in both directions enabling a 180° reach. The Pulse Width Modulation signals which are used for the operational control of the servo motor is processed faster and more efficiently. It is equipped with a complex internal circuit which gives high torque and better stability. Connection pin specification is shown in table 3.4.

Table 3.4 Pin specification of DC Servo motor

Pin	Name	Function
1	Signal pin (Orange pin)	The PWM signal which states the axis position is given through this pin.
2	VCC (Red pin)	Positive power supply for servo motor is given to this pin.
3	Ground(Brown pin)	This pin is connected to ground of circuit or power supply.

3.4.4 Bluetooth Module HC-05

The HC-05 Bluetooth Module can be enabled both as Master and slave (Figure 3.7). The Master setting enables auto-communication between two Bluetooth devices whereas the slave set can only accept incoming connections. It has a 3Mbps data transmission speed with a 2.4 Giga hertz transmitter and receiver (Table 3.5). It comprises of six pins, V_{cc} – for power supply; G_{nd} – for negative; T_x – for transmission; R_x – for receiving; a Key to switch between Master and Slave and LED to display its operational activity.

Table 3.5 Specification of Bluetooth Module HC-0. Source: - www.electronicaestudio.com

Sr. No.	Features	Description
1	Protocol	Bluetooth Specification v2.0+EDR
2	Frequency	2.4GHz ISM band
3	Modulation	GFSK
4	Emission power	≤4dBm, Class 2
5	Sensitivity	≤-84dBm at 0.1% BER
6	Speed	Asynchronous: 2.1Mbps/ 160 kbps, Synchronous: 1Mbps/1Mbps
7	Security	Authentication and encryption
8	Profiles	Bluetooth serial port
9	Power supply	+3.3VDC 50mA
10	Working temperature	-20 ~ +75 °C

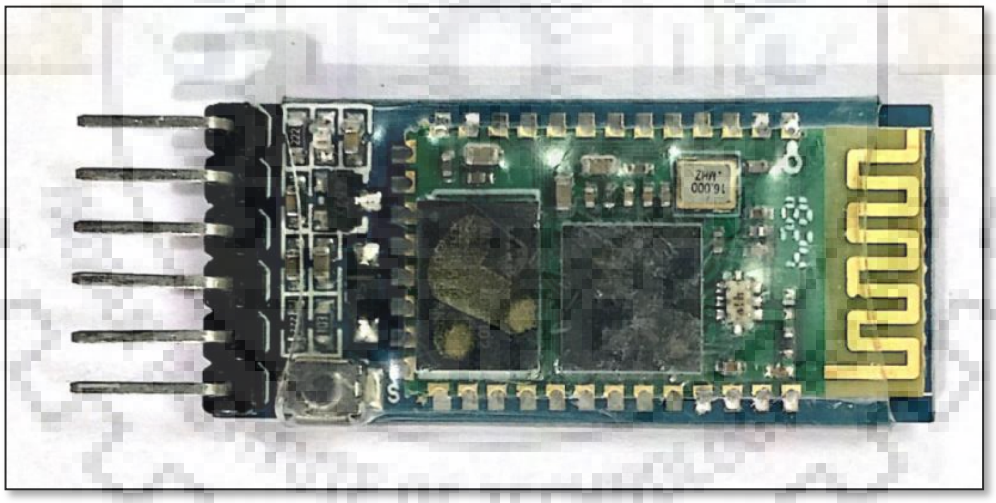

Figure 3.7 HC-05 Bluetooth Module

3.4.5 Motorized Globe Valve

A motorized globe valve has been employed to control the bypass flow to maintain a constant pressure in the main line which works through a pressure feedback circuit from main line. A 2-way globe valve of metal to metal seating having a constant total flow throughout the full plug flow provides linkages to strain relief mechanism to assure tightest close-off with minimal strain on the motor (Table 3.6). It has an intelligent circuit that senses hindrance in valve movements. AC sensor is used for circuit protection and it can shut down the valve during an overload condition. It has a robust and compact design for ease of installation (Figure 3.8).

Table 3.6 Specification of 2-way motorized globe valve. Source: - www.rohtashsons.com

Sr. No.	Features	Description
1	Body Test Pressure	21 kg/cm2
2	Working Pressure	7 kg/cm2
3	Voltage	24V AC/DC
4	Actuator	RS
5	Size	50 mm
6	Brand	CI
7	Ambient Temperature	Min- 1oC, Max- 80oC
8	Material	Cast Iron IS210 FG260
9	End	Screwed Ends, Flanged End
10	Actuator Type	Pressure Die Casted
11	Power Supply	24 V AC
12	Temperature (deg. Celsius)	1oC-80oC
13	Control Type	Modulating 4-20 mA Control Signal
14	Body Material	Cast Iron
15	Plug And Seat	Brass IS1264, great DCB-I

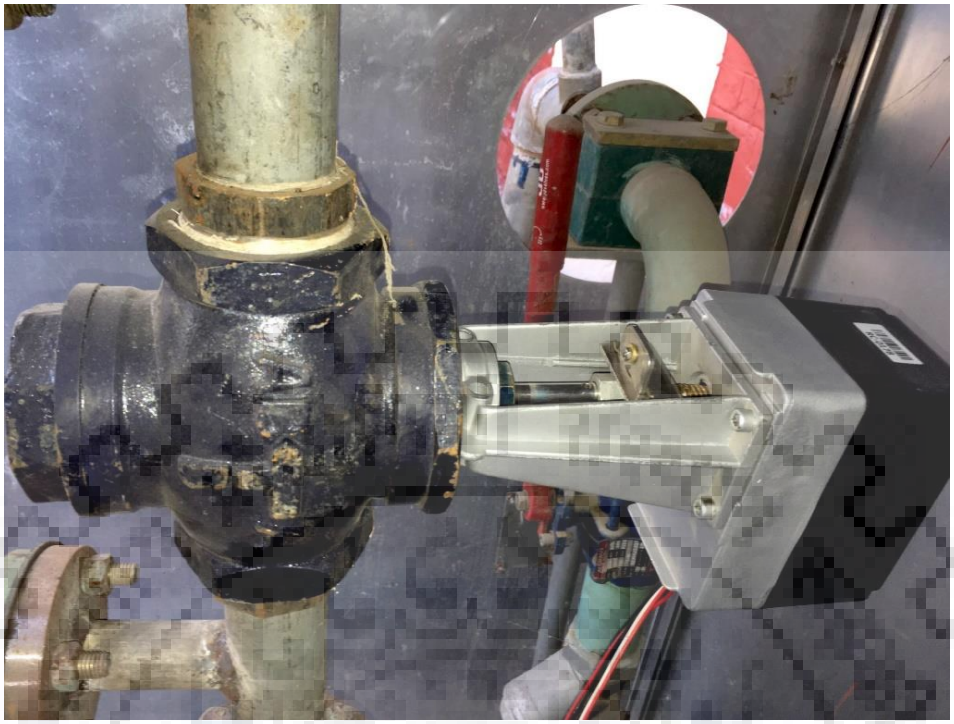

Figure 3.8 Motorized globe valve

3.4.6 Pressure Transmitter

The mass PT11 pressure transmitter has a very compact design with stainless steel construction (Figure 3.9). It is highly stable against shock and vibration and also have features such as reverse polarity, limit protection and have high accuracy (Table 3.7). This pressure sensor is installed to check the main line pressure. PID controller can sense the change in pressure and can act accordingly to operate bypass and to maintain a constant pressure in main line for an uniform rainfall intensity.

Table 3.7 Specifications of Pressure sensor PT11. Source: - www.precisionmass.com

Sr. No.	Technical specifications	PT11	
1	Measuring principle	Piezo resistive sensors	
2	Range in bar	0-6	
3	Overpressure limit	-1/0 -1/3 -1/5 -1/9 -1/15	
4	Pressure type	Gauge	
5	Process connection	G 1/4 male according to DIN 3852 Part 11 Form E	
6	Material Wetted Part	Stainless Steel 316L	
7	Process connection	Stainless Steel 316L	
8	Sensor Housing	Stainless Steel 300 series	
9	Seals	FKM	
10	Power supply	11- 28 VDC	
11	Output signal	4 - 20 mA (2 wires)	0 - 5 VDC (3 wires)
12	Maximum Loop Resistance	(U – 12V)/0.02 Ω	
13	Insulation Voltage	100V,100MΩ	
14	Electrical connection	4 PIN angle connector DIN EN 175301-803 A, DIN EN 175301-803 C (IP65)	
15	Accuracy	≤ 0,5 % FS, optional ≤ 0,25 % FS	
16	Long term stability	≤0,2 % FS / year	
17	Operation temperature	-20 - 80 °C	
18	Medium temperature	-40 - 125 °C	
19	Storage temperature	-25 - 85 °C	
20	Vibration resistance	10gRMS, （20～2000）Hz	
21	Shock resistance	100g, 11ms	
22	Protection acc. EN 60 529/IEC 529	IP67 / IP65	
23	Weight in kg	~ 0.20	

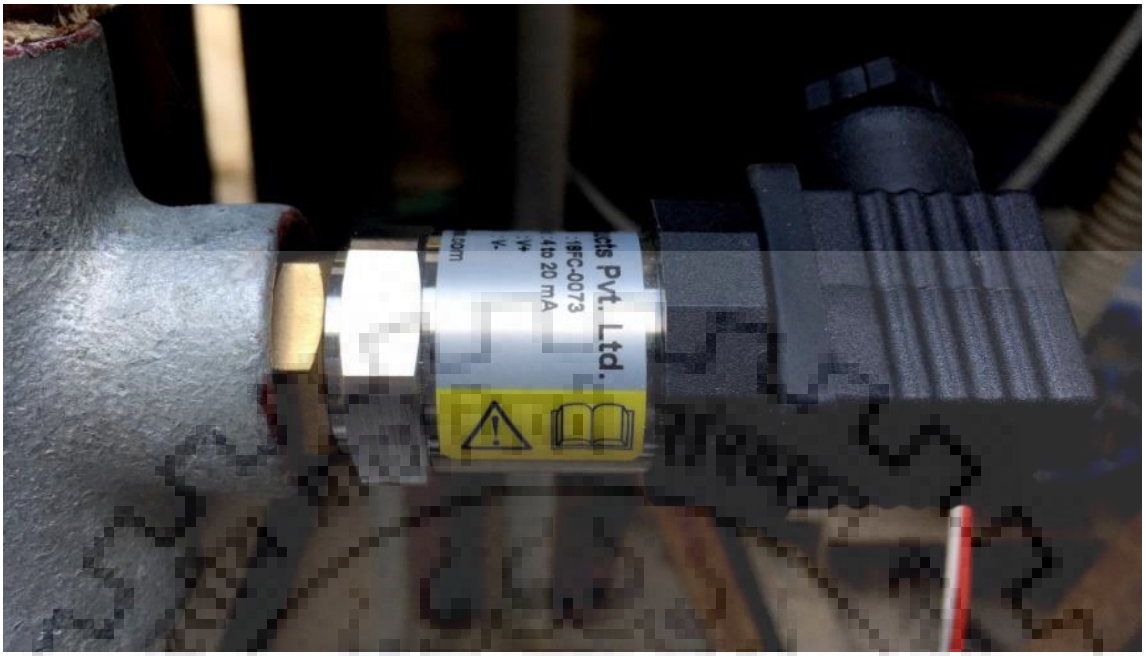

Figure 3.9 Pressure sensor PT11

3.4.7 Selec PID500

Selec PID500 is a controller which is employed widely in industrial process controls. PID controller is used to operate a motorized globe valve on the basis of an input signal from a pressure sensor. Whenever there is a pressure offset from the set value, it sends a signal to the motorized valve to re-attain the set value. The I/O signal from the pressure sensor and PID respectively ranges between 4-20 mA (Table 3.8). The controller has a compact square housing with panel mounting facility in its enclosure, powered by a 240 V AC supply (Figure 3.10). PID controller is used to control bypass flow by operating a motorised valve to maintain constant pressure in the main line against any pressure drop generated due to the moving storm simulation.

Table 3.8 Specification of Selec PID500. Source: - www.selec.com

Sr. No.	Technical specifications	Selec PID-500
1	Display Type	7 Segment LED Dual Display
2	Display Configuration	4+4 digits
3	Type of Inputs	Signal Inputs: (DC) -5 to 56mV, 0 to 10V, 0 to 20mA
4	Control Output	Current : 4 to 20mA DC or Voltage :0 to 10V DC
5	Auxiliary Output	Relay
6	Feature	Extra alarm output, Retransmission output
7	Communication	RS485 MODBUS communication
8	Supply Voltage	85 to 270V AC / DC
9	Size	48 x 48mm
10	Mounting Type	Panel Mount
11	Certification	CE, UL

Figure 3.10 Selec PID500

3.5 Circuit Design and Coding

The circuit design comprises of an Arduino mega (AM), Bluetooth module (BM) HC-05 and 11 servo motor operated valves. The four connections, R_x, T_x, V_{cc} and G_{nd} in the BM is connected to the recipient ports in the AM, pin 11, pin 10, 3.3 V and G_{nd} respectively. The 11 servos are grouped into four sets like 3, 3, 3 and 2 each in each group. The signal pins of these groups of servo motors are connected to the digital signal pins of AM, numbered as pin 3, pin 5, pin 6 and pin 9. Each group has a power supply of 5 V – 2 A and they are in turn grounded to AM which has a power supply of 12 V – 1 A (Figure 3.11). The AM has been coded in a way that it can be regulated with any android based phone through a Bluetooth application to control all the motors simultaneously. Two basic C/C++ microcontroller libraries have been used "SoftwareSerial.h' and "Servo.h" in this code but one can modify the code as per their own utility. The software used to write the code is Arduino Editor and this software is also available online.

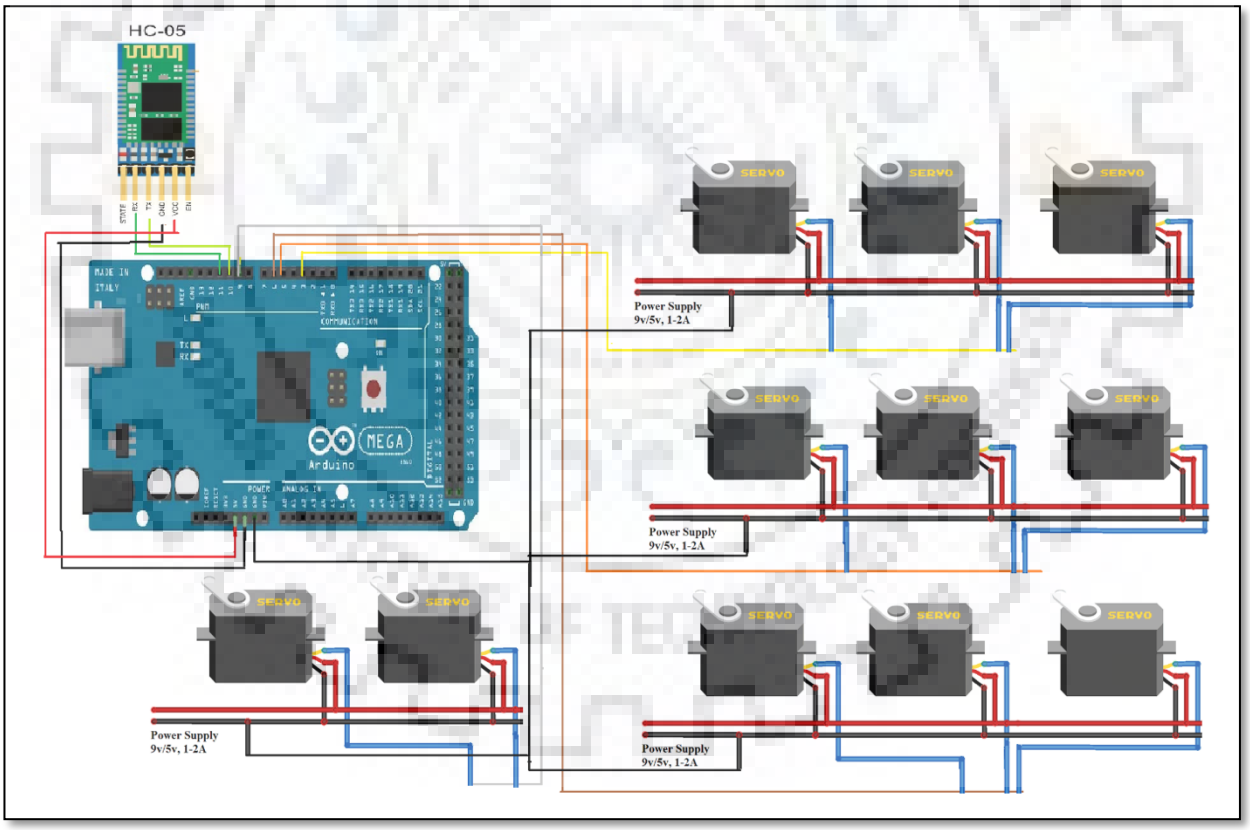

Figure 3.11 Circuit diagram

3.5.1 User Interface

An Android phone application is designed for users to operate all 11 nozzles simultaneously (Figure 3.12). It can be operated with one touch Bluetooth connectivity and four slider bar to control for groups of servo operated valves at any group of values ranging from 0 to 100 percent. This application is developed in software named as “MIT app developer”.

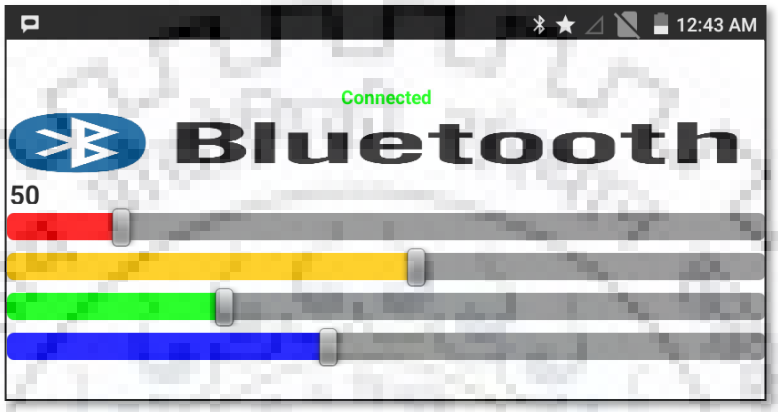

Figure 3.12 Screenshot of User interface

The brief descriptions of all the hardware used in moving storm rainfall simulator are discussed below.

Table 3.9 Specification for components used for moving storm rainfall simulator

Sr. No.	Component	Specification	Quantity	Utility
1	Arduino	Mega	1	To control servo motors
2	Servo motor	MG995 Tower-Pro	11	To operate valve
3	Bluetooth module	HC-05	1	To receive signal from mobile
4	Valves	Stop Cock 15 mm	11	To control flow
5	Hexagonal nipple	15 mm	11	Connect valves to main frame
6	Power supply	12 V 1 Amp	1	Power supply for Arduino mega
		5 V 2 Amp	4	Power supply for servo
7	Motorized globe valve	2 inch	1	To control bypass flow
8	Selec PID	PID500	1	To control motorized globe valve on basis of pressure
9	Pressure sensor	PT11	1	To sense pressure in main line

3.6 Design of Experimentation

Experiments are designed in such a systematic way that with a minimum number of simulations a simplified and efficient result can be achieved (Table 3.9). Three replications of each scenario are conducted to increase the confidence in the results. Experiments are performed with three different speeds (2 m/min, 3 m/min and 6 m/min), two different slope conditions (2.5% and 5%) and two directions of storm movement (downslope to upslope and vice versa). Experiments are done under fully saturated soil bed condition, to keep each simulation comparable (Table 3.9).

Table 3.10 Design of experimentation

No. of scenarios	Slope (%)	Storm velocity (m/min)	Storm direction
1	2.5	2	Upstream
2	2.5	2	Downstream
3	2.5	3	Upstream
4	2.5	3	Downstream
5	5	2	Upstream
6	5	2	Downstream
7	5	3	Upstream
8	5	3	Downstream
9	5	6	Upstream
10	5	6	Downstream

Chapter 4

RESULTS AND DISCUSSION

Figure 4.1 shows the 3D visualization of rain intensity over the entire catchment at an instant of time. Spatial distribution of simulated rainfall through the nozzles over the catchment. As per the Christiansen Uniformity Coefficient (CU) calculation, rainfall uniformity was 84%.

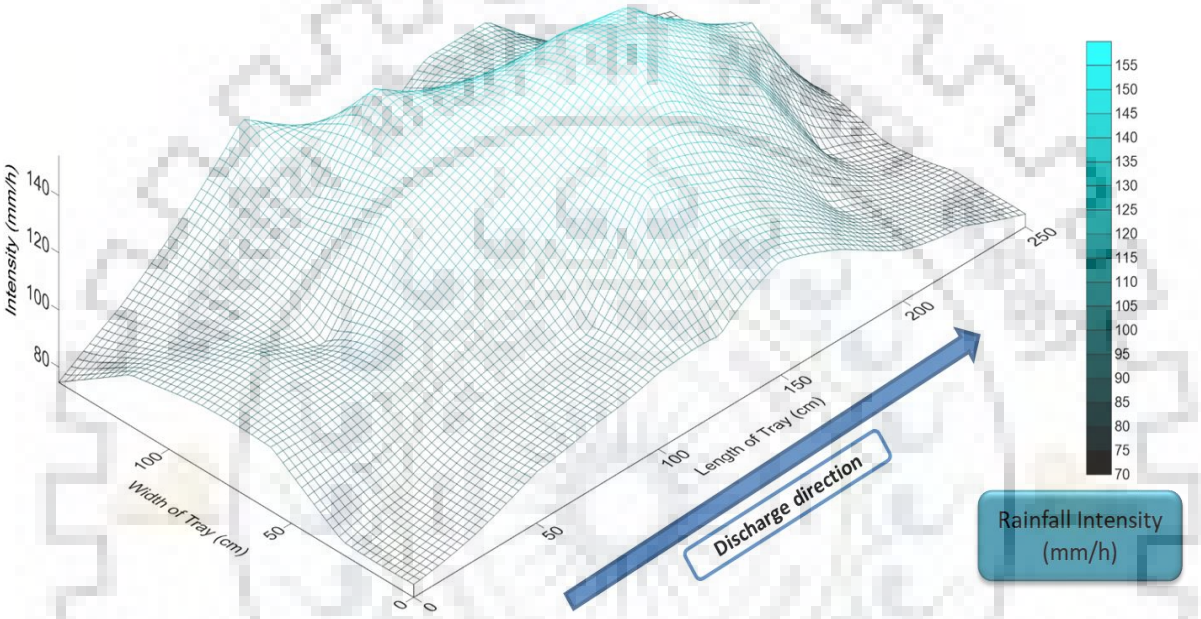

Figure 4.1 3D-rainfall distribution graph

4.1 Results for experimentation conducted at 2.5% slope

The results recorded by moving storm rainfall simulator clearly show the effect of storm direction, velocity and slope on overland flow hydrographs. Considering the storm movement direction of both downstream and upstream with storm movement velocity of 2 m/min at a slope of 2.5% produced hydrographs as shown in Figure 4.2. The time to peak of hydrograph generated by upstream to downstream storm is less than the downstream to upstream storm. It can be seen from Figure 4.2 that the time to peak is 50 sec while the storm is moving from upstream to downstream and it is increased up to 100sec during the opposite storm movement condition. The hydrograph produced by downstream to upstream storm movement shows longer recession time comparison to the upstream to downstream storm. When the storm is moving towards the downstream

direction, it shows higher peak comparison to the upstream direction movement. The downstream directional storm produced a peak flow of 0.0086 l/s whereas upstream directional storm produced 0.0065 l/s peak discharge (Table 4.1). Similar characteristics of peak time and peak discharge are also found for 3m/min storm movement velocity. Storm velocity of 3 m/s shows a peak discharge of 0.0047 l/s and 0.003 l/s during downstream and upstream directional storm movement, respectively. However, a negligible change in recession time is observed between both the storm directions during 3 m/min storm velocity (Figure 4.3). It can be seen from Table 4.1 that storm velocity of 2m/min produces more runoff volume in comparison to 3m/min. When the storm is moving in the downstream direction, 2m/min storm velocity shows a longer recession time comparison to 3m/min velocity. However, when the storm is moving towards upstream direction no such change in recession time is observed between both the velocity conditions i.e. 2m/min and 3m/min.

Table 4.1 Variation of hydrograph parameter's considering different storm velocity at slope 2.5%

Velocity	2 m/min		3 m/min	
	Downstream	Upstream	Downstream	Upstream
Time to peak (sec)	50	100	50	80
Peak runoff (l/sec)	0.0086	0.0065	0.0047	0.003
Runoff volume (L)	0.913	1.080	0.4767	0.3606

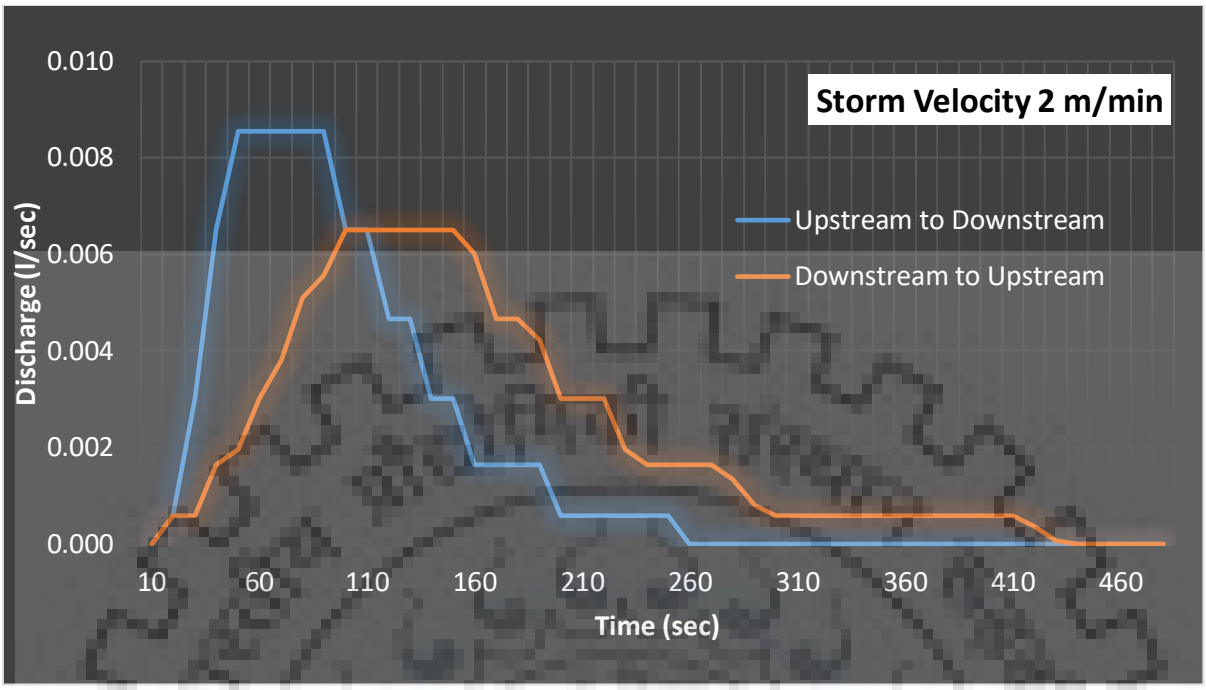

Figure 4.2 Hydrograph for velocity 2 m/min at 2.5% slope.

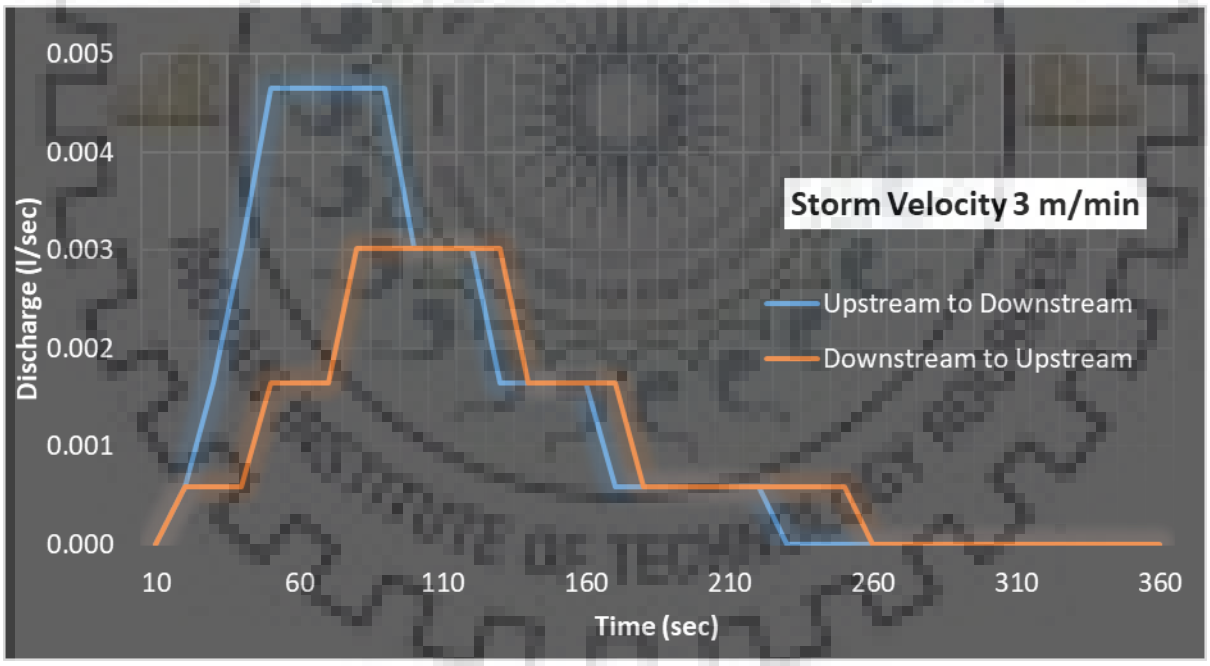

Figure 4.3 Hydrograph for velocity 3 m/min at 2.5% slope.

4.2 Results for experimentation conducted at 5% slope

At 5% slope condition, rainfall simulation experiments are performed with three different velocities 2 m/min, 3 m/min and 6 m/min, and storm movement directions are taken same as the previous experiment i.e. upstream and downstream. It can be clearly illustrated from figures 4.4 & 4.5 that the recession characteristics, time to peak and peak discharge follows the same trend as the 2.5% slope hydrograph characteristics. An interesting observation is noticed during testing of 6m/min storm velocity i.e. the recession curve and peak discharge of both hydrographs completely matched with each other during upstream & downstream directional storm movement. Only time to peak is varied in these two hydrographs of 6m/min velocity storm.

It can be observed from Table 4.1 and 4.2 that as the slope increases, the time to peak value decreases when the storm is moving from downstream to the upstream direction. But the time to peak is remaining constant when the storm is moving towards downstream. While moving towards downstream direction at a velocity of 2m/min, the peak runoff value for 5% slope is found to be 0.016 l/s which is 53.7 % higher than 2.5% slope condition. Similarly, for 3m/min velocity, the peak discharge of 5% slope is 43.3 % higher than the 2.5% slope. When moving towards upstream direction at a velocity of 2m/min and 3m/min, the peak runoff of 5% slope is 59% and 42.8% higher than the 2.5% bed slope condition, respectively. The runoff volume resulted from 3% flume slope 67.38% greater than the 2.5% slope when the storm is moving towards the outlet at a velocity of 2m/min. While moving towards the upstream direction, the runoff volume of 5% slope increased up to 82% comparison to 2.5% slope. Similarly, for 3m/min velocity, the increase in flow volume due to slope increment is 58.56% and 55.56% for downstream and upstream storm direction, respectively.

As the storm is moving in downstream direction i.e. towards the outlet, it shows a quick rise in hydrograph and delayed low peak. Peak runoff is observed at outlet only when entire catchment contributes, this is possible only when the storm reaches the upstream point. As a result longer time is required to attain the peak. This is evident from the lag of the hydrograph. Contrast to this, when storm direction is reversed i.e. storm is moving to upstream, the runoff is initiated at the upstream point and flows downstream end along with the storm, thus collective runoff reaches outlet at the same time which results in a sharp peak at the outlet of the soil flume. Similar

experimental results are also found in the study of de Lima and Singh (2003, 2007 & 2009) in which they used a 1.25m wide and 5m long impermeable plane for moving storm experiment. Ren et al. (2013) used hypodermic needles for moving storm experiment and also found similar kind of results.

Table 4.2 Variation of hydrograph parameter's considering different storm velocity at slope 5%.

Velocity	2 m/min		3 m/min		6 m/min	
	Downstream	Upstream	Downstream	Upstream	Downstream	Upstream
Time to peak (sec)	50	70	50	60	20	30
Peak runoff (l/s)	0.016	0.011	0.011	0.007	0.0016	0.0016
Runoff volume (L)	1.355	1.320	0.814	0.649	0.215	0.194

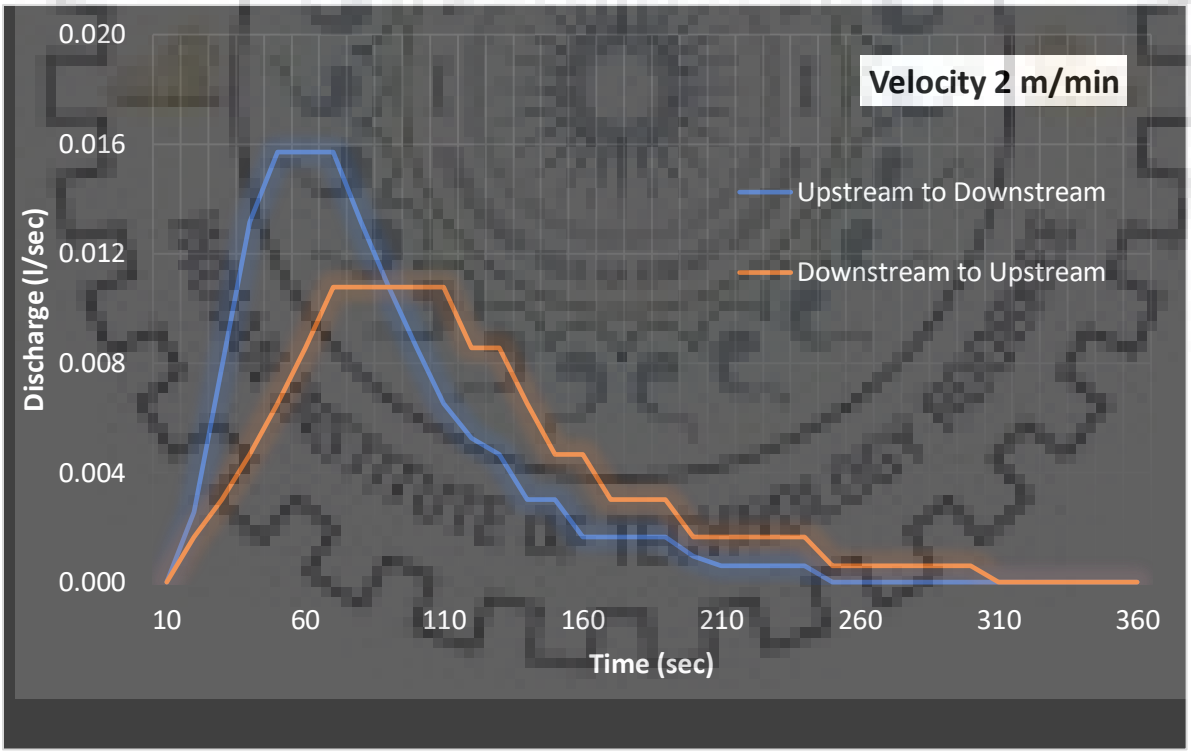

Figure 4.4 Hydrograph for velocity 2 m/min at 5% slope.

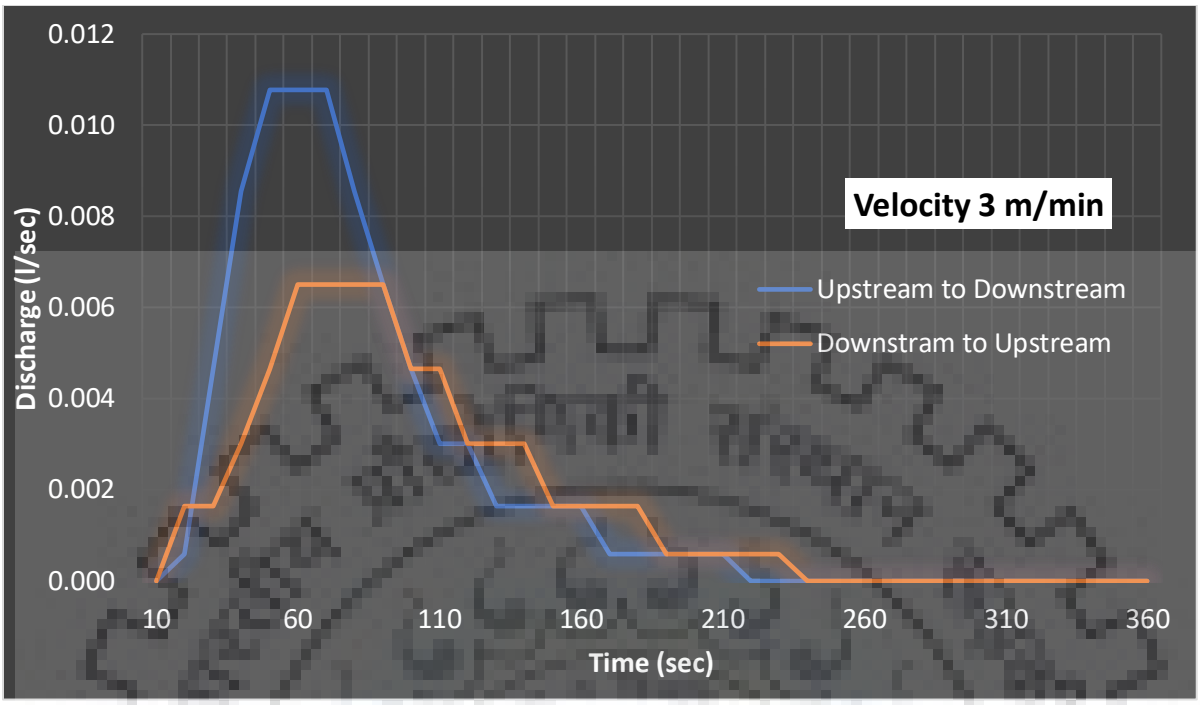

Figure 4.5 Hydrograph for velocity 3 m/min at 5% slope.

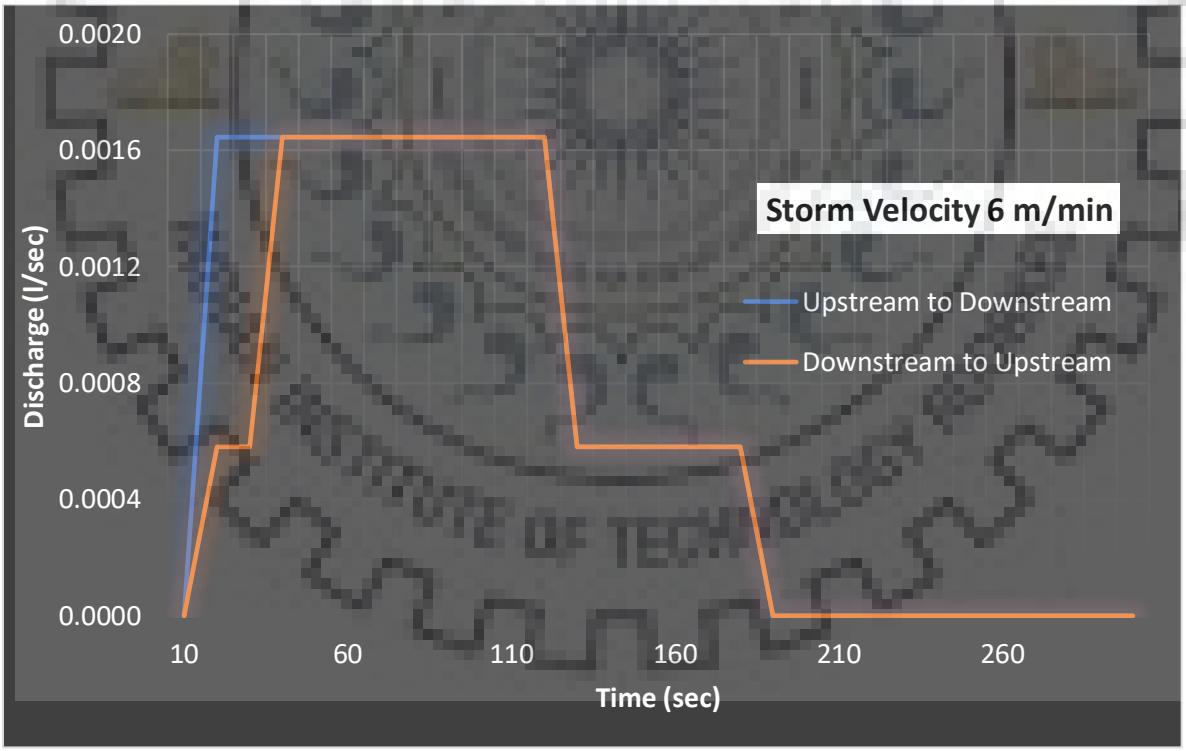

Figure 4.6 Hydrograph for velocity 6 m/min at5% slope.

Chapter 5
CONCLUSIONS

The hydrographs are developed using moving storm rainfall simulator on a saturated soil surface. The results indicate a significant influence of spatial and temporal distributions of rainfall on hydrograph and its characteristics. In the experiments, storm movement is considered along the slope of the basin in both the directions with two different bed slope and three different velocities, rest all other parameters were kept constant (e.g., rainfall intensity, soil saturation).

Following conclusions were drawn from the study:

1. The hydrograph generated from downstream moving storms yielded higher peak with a sharp rise and short recession limb.
2. The upstream moving storm i.e against the flow direction produced a hydrograph with lower peak and a prolonged gradually decreasing recession limb.
3. With an increase in storm movement velocity, the impact of moving storm phenomenon in terms of peak discharge and time to peak becomes negligible. This was true for both the directions.
4. Similarly, an increase in the basin slope reduced the impact of moving storm on overland flow.

5.1 Future scope

This study is limited to evaluating the impact of storm movement on generated hydrograph under single storm pattern with two different slope condition, two different storm direction and three different velocity. This advance rainfall simulator design can used to analyze the impact of storm movement over soil erosion and nutrition transport. Flume designed for this study can be used for subsurface flow, base flow and leachate experiments.

REFERENCES

Cai, J., Li, P., Wang, P., 2012. An approach to rainfall simulator automation and performance evaluation. Proc. World Congr. Intell. Control Autom. 3428–3433. https://doi.org/10.1109/WCICA.2012.6359040

De Lima, J.L.M.P., Dinis, P.A., Souza, C.S., De Lima, M.I.P., Cunha, P.P., Azevedo, J.M., Singh, V.P., Abreu, J.M., 2011. Patterns of grain-size temporal variation of sediment transported by overland flow associated with moving storms: Interpreting soil flume experiments. Nat. Hazards Earth Syst. Sci. 11, 2605–2615. https://doi.org/10.5194/nhess-11-2605-2011

de Lima, J.L.M.P., Singh, V.P., 2003. Laboratory experiments on the influence of storm movement on overland flow. Phys. Chem. Earth 28, 277–282. https://doi.org/10.1016/S1474-7065(03)00038-X

De Lima, J.L.M.P., Singh, V.P., 2002. The influence of the pattern of moving rainstorms on overland flow. Adv. Water Resour. 25, 817–828. https://doi.org/10.1016/S0309-1708(02)00067-2

De Lima, J.L.M.P., Singh, V.P., De Lima, M.I.P., 2003. The influence of storm movement on water erosion: Storm direction and velocity effects. Catena 52, 39–56. https://doi.org/10.1016/S0341-8162(02)00149-2

de Lima, J.L.M.P., Tavares, P., Singh, V.P., de Lima, M.I.P., 2009. Investigating the nonlinear response of soil loss to storm direction using a circular soil flume. Geoderma 152, 9–15. https://doi.org/10.1016/j.geoderma.2009.05.004

Egodawatta, P., Thomas, E., Goonetilleke, A., 2009. Understanding the physical processes of pollutant build-up and wash-off on roof surfaces. Sci. Total Environ. 407, 1834–1841. https://doi.org/10.1016/j.scitotenv.2008.12.027

Hall, M.J., 1970). A critique of methods of simulating rainfall. Water Resour. Res., 6(4): 104-114

Herngren, L., Goonetilleke, A., Sukpum, R. and de Silva, D.Y., 2005. Rainfall Simulation as a Tool for Urban Water Quality Research. Environmental Engineering Science. 22 (3), 378-383

Lee, T., Shin, J., Park, T., Lee, D., 2015. Basin rotation method for analyzing the directional influence of moving storms on basin response. Stoch. Environ. Res. Risk Assess. 29, 251–263. https://doi.org/10.1007/s00477-014-0870-y

Liu, A., Egodawatta, P., Guan, Y., Goonetilleke, A., 2013. Influence of rainfall and catchment characteristics on urban stormwater quality. Sci. Total Environ. 444, 255–262. https://doi.org/10.1016/j.scitotenv.2012.11.053

Meyer LD, McCune DL. 1958. Rainfall simulator for runoff plots. Agricultural Engineering 39: 644-648

Miguntanna, N.P., Goonetilleke, A., Egodowatta, P., Kokot, S., 2010. Understanding nutrient build-up on urban road surfaces. J. Environ. Sci. 22, 806–812. https://doi.org/10.1016/S1001-0742(09)60181-9

Norris P. Swanson, 2013. Rotating-Boom Rainfall Simulator. Trans. ASAE 8, 0071–0072. https://doi.org/10.13031/2013.40430

Ran, Q., Shi, Z., Xu, Y., 2013. Canonical correlation analysis of hydrological response and soil erosion under moving rainfall. J. Zhejiang Univ. Sci. A 14, 353–361. https://doi.org/10.1631/jzus.a1200306

Regmi, T.P., Thompson, A.L., (2000). Rainfall simulator for laboratory studies. Applied Engineering in Agriculture 16, 641-652

Romkens, M., Roth, C.B.N.D.W., 1977. Erodibility of Selected Clay Subsoils in Relation to Physican and Chemical Properties. Soil Sci.Am.J. 41, 954–959.

Seo, Y., Schmidt, A.R., 2014. Evaluation of drainage networks under moving storms utilizing the equivalent stationary storms. Nat. Hazards 70, 803–819. https://doi.org/10.1007/s11069-013-0845-1

Seo, Y., Schmidt, A.R., 2012. The effect of rainstorm movement on urban drainage network runoff hydrographs. Hydrol. Process. 26, 3830–3841. https://doi.org/10.1002/hyp.8412

Sigaroodi, S.K., Chen, Q., 2016. Effects and consideration of storm movement in rainfall-runoff

modelling at the basin scale. Hydrol. Earth Syst. Sci. 20, 5063–5071. https://doi.org/10.5194/hess-20-5063-2016

Singh, R., Panigrahy, N., Philip, G., (1999). Modified rainfall simulator infiltrometer for infiltration, runoff and erosion studies. Agric. Water Manage. 41, 167-175

Wilson, C.B., Valdes, J.B., Rodriguez-Iturbe, I., 1979. On the influence of the spatial distribution of rainfall on storm runoff. Water Resour. Res. 15, 321–328. https://doi.org/10.1029/WR015i002p00321